Characterization of post-translational modification of ATG16L1 in antibacterial autophagy

Reham Alsaadi

Thesis submitted to the Faculty of Graduate and Postdoctoral Studies in partial fulfillment of the requirements for the degree of Master of Science, Cellular and Molecular Medicine

Department of Cellular and Molecular Medicine

Faculty of Medicine

University of Ottawa

Abstract

Autophagy is a highly regulated catabolic pathway that is potently induced by stressors including starvation and infection. An essential component of the autophagy pathway is an ATG16L1-containing E3-like enzyme, which is responsible for lipidating LC3B and driving autophagosome formation. ATG16L1 polymorphisms have been linked to the development of Crohn's disease (CD) and phosphorylation of CD-associated ATG16L1 (caATG16L1) has been hypothesized to contribute to cleavage and autophagy dysfunction. Here we show that ULK1 kinase directly phosphorylates ATG16L1 in response to infection and starvation. Moreover, we show that ULK1-mediated phosphorylation drives the destabilization of caATG16L1 in response to stress. Additionally, we found that phosphorylated ATG16L1 was specifically localized to the site of internalized bacteria indicating a role for ATG16L1 in the promotion of anti-bacterial autophagy. Lastly, we show that stable cell lines harbouring a phospho-dead mutant of ATG16L1 have impaired xenophagy. In summary, our results show that ATG16L1 is a novel target of ULK1 kinase and that ULK1-signalling to ATG16L1 is a double-edged sword, enhancing function of the wildtype ATG16L1, but promoting degradation of caATG16L1.

Table of Contents

List of Figures

List of Table

List of Abbreviations

AMP	Adenosine monophosphate
AMPK	AMP-activated protein kinase
AR	Autoradiography
ATG	Autophagy-related
ATP	Adenosine Triphosphate
BECN1	Beclin 1
caATG16L1	CD-associated ATG16L1
CD	Crohn’s disease
CFU	Colony Forming Unit
CTEP	2-chloro-4-[2-[2,5-dimethyl1-[4-(trifluoromethoxy)phenyl]imidazol-4-yl]ethynyl]pyridine
dKO	Double knockout
DMEM	Dulbecco's Modified Eagle'smedium
ER	Endoplasmic reticulum
FIP200	Focal adhesion kinase family interacting protein of 200kD
GWAS	Genome-wide association studies
HCT116	Human colorectal carcinoma cell line.
HD	Huntington’s disease
HEK293A	Human embryonic kidney cells 293
Htt	Huntingtin protein

IF	Immunofluorescent
IKKα	IκB kinase subunit
IRGM	Immunity related GTPase M
KO	Knockout
LC3	Microtubule-associated proteins 1A/1B light chain 3
LPS	Lipopolysaccharide
MCF7	Michigan Cancer Foundation-7
MEF	Mouse embryonic fibroblasts
mGluR5	Metabotropic glutamate receptor 5
MNV	Murine noroviruses
MOI	The multiplicity of infection
mTORC1	The mammalian target of rapamycin complex 1
NDP52	Nuclear Domain 10 Protein 52
NOD2	Nucleotide-binding oligomerization domain-containing protein 2
p62/SQSTM1	Sequestosome 1
PFA	Paraformaldehyde
PtdIns 3-kinase	phosphatidylinositide 3-kinases
R848	Resiquimod
RB1CC1	RB1-inducible coiled-coil protein 1
SCV	Salmonella-containing vacuoles
SNP	Single nucleotide polymorphism

STK11 /LKB1	Liver kinase B1
TLR4	Toll-like receptor 4
TSC2	Tuberous sclerosis 2
UC	ulcerative colitis
ULK	unc-51-like kinase
UPR	Unfolded protein response
UVRAG	UV irradiation resistance-associated gene
VMP1	Vacuole membrane protein 1
VPS34	Vacuolar protein sorting
WB	Western blot
WIPI	WD-repeat protein interacting with phosphoinositides

Acknowledgments

After an intensive period of two years, today is the day to write the finishing touch on my thesis. It has been a great time for me, both academically and personally. I would like to express my very heartfelt appreciation to the people who have supported and helped me so much throughout these two years. It is hard to overstate my gratitude to my thesis supervisor, Dr. Ryan Russell for his unending support, guidance and tutelage. Dr. Russell put tremendous efforts to explain things to me clearly and simply. Science became even more fun for me under his supervision. He encouraged me all time, gave sound advices, and never runs out of incredible ideas, I would have been lost without him.

I would like to thank the Thesis Advisory Committee Dr. Laura Trinkle-Mulcahy and Dr. Marceline Côté for their constructive criticisms that helped build and improve my skills as a scientist. I am especially grateful to lab mates Wensheng, Cloe, Zhihao, Yujin, Mercy and Karyn for providing an exciting and fun environment for learning and growing.

I am dedicating my thesis to my parents, for their love and constant support; my mother, Aisha Saleh Alsaadi, the most incredible woman I know. Thank you for sacrificing your dreams in order to help us achieving ours. Thank you for having faith in my goals and standing with me in all of my decisions; my Father, Musaibeh Muaad Alsaadi, thank you for pushing me to study so hard for the last 17 years, you are the reason why I am in love with school and especially science. Thank you for believing in my dreams and helping me actualize them. There are not enough words to express my appreciation for you; my siblings, Abeer, Ahlam, Nawal, Maram, Muhammed, Khaled, Abdallah, Ziyad, and Rawah you all are the most wonderful gift I ever had. Thank you for being there whenever I needed you or not. Thank you all for being the greatest support system I could ever wish for. Nawal and Ahlam thank you for helping me since day one in Canada. Honestly, it would have been way harder without you here with me. I love you all and I appreciate your existence in my life.

Sources of Funding

This work was supported by Canadian Institutes of Health Research (CIHR) Project Grants awarded to Ryan Russell (#PJT153034).

Introduction

Macroautophagy (hereafter referred to as autophagy) is a cellular degradative process capable of degrading a vast array of substrates including cytoplasm, organelles, aggregated macromolecules, and pathogens[1]. Degradation of autophagic cargo occurs after sequestration of cargo in a double-membraned vesicle called an autophagosome, which matures into a degradative vesicle after fusion with lysosomes[1]. Autophagy can be activated by multiple cellular stresses including nutrient depletion, hypoxia, and infection by pathogens [2]. Autophagy defects have been linked to human pathophysiology in an array of common diseases, such as neurodegeneration, autoimmunity, cancer[3].

History of Autophagy

Autophagy was first discovered in 1963 by Christian de Duve who utilized electron microscopy to study the fine inner structures of the cell[4]. In these experiments he identified a novel double-membrane vesicle containing sequestered cytoplasmic cargo, which he named “autophagosomes” [5]. Additionally, he coined the term “autophagy”, from the Greek roots *auto* “self” and *phagy* “eating”[1]. For determining the structural organization of the cell, he shared the Nobel Prize in Physiology or Medicine in 1974. Until the 1990s, research in the autophagy field was mainly observational and morphological-based and the importance of the pathway was not appreciated[4]. However, in 1993, Yoshinori Oshumi conducted a genetic screen in yeast under nitrogen starvation that resulted in the isolation of autophagy-defective mutants, which were known as ATG (Autophagy-related) genes[6]. The genetic screens led to the discovery of mutants composed of 15 complementation groups, indicating that at least 15 genes were

implicated in the regulation of autophagy in yeast upon nutrient deprivation[7]. Today, 41 yeast ATG genes have been characterized and many of these have homologs in humans[8]. Ohsumi and his colleagues' efforts to characterize the genetic basis of autophagy led to a surge in autophagy research and in 2016 Oshumi was awarded the Nobel Prize in Physiology or Medicine in 2016 for his landmark discovery of yeast autophagy-related (ATG) genes[9].

Autophagosome Biogenesis

The physical process of autophagy begins with the nucleation of a small double-membraned structure called the phagophore, which is believed to be of either ER or endosomal origin. This small cup-shaped membrane serves as the initiation center of autophagosome formation. It recruits multiple ATG proteins that assist the elongation of the phagophore to eventually encircle the autophagic cargo to form the autophagosome. The mature autophagosome then fuses with lysosome, resulting in the formation of the degradative autolysosome. Lysosomal proteins located on the membrane function to acidify the lumen activating the acid hydrolases to degrade the entire autophagosome together with its cargo[10] (Fig.1).

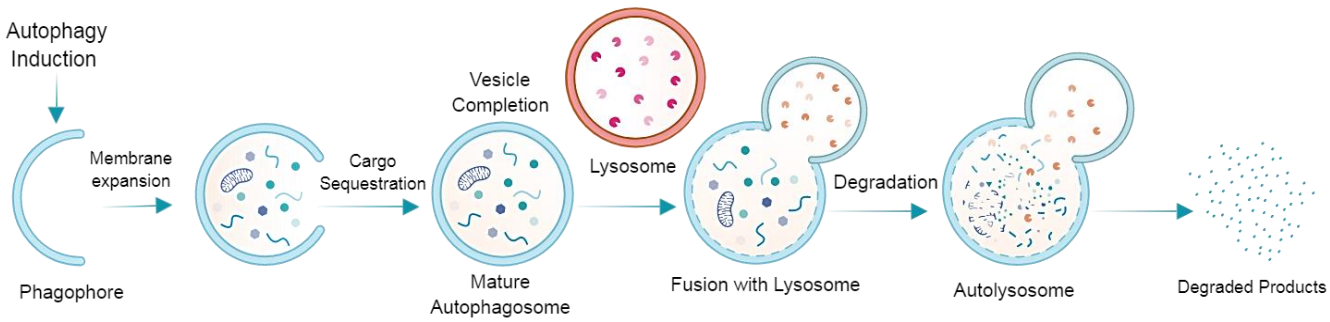

Figure 1: Model for the biogenesis and maturation of an autophagosome.

Core Molecular Machinery

Significant advances have been made in yeast and mammalian cells on understanding the mechanisms of autophagosome formation. These advances were mainly dependent on the identification of autophagy-related (ATG) proteins that were originally found in yeast (Table.1). These ATG proteins were found to function in several major functional classes in the promotion of autophagy including: i) the ATG1/unc-51-like kinase (ULK) complex, ii) the class III PtdIns 3-kinase PIK3C3/VPS34 complex I, iii) transmembrane proteins including ATG9, iv) WIPI proteins, v) and two ubiquitin-like protein conjugation systems (ATG12–ATG5-ATG16L1 and the mammalian ortholog of yeast Atg8, MAP1LC3 (LC3)) to facilitate the progression of autophagy[11].

	Yeast	Mammal	Characteristics
Atg1/ULK kinase complex	Atg1	ULK1/2	Serine/threonine protein kinase
	Atg13	ATG13	Regulator of the Atg1 complex through phosphorylation
	Atg17	RB1CC1/FIP200 (functional homolog)	Component of the Atg1 complex
	Atg29		Component of the Atg1 complex
	Atg31		Component of the Atg1 complex
		C12orf44/ATG101	Component of the ULK complex in mammals
Atg9 and its cycling system	Atg2	ATG2	Peripheral membrane protein
	Atg9	ATG9	Transmembrane protein
	Atg18	WIPI1/2	Peripheral membrane protein
Class III PtdIns3K complex	Vps15	PIK3R4/VPS15/p150	Serine/threonine protein kinase
	Vps34	PIK3C3/VPS34	PtdIns3K
	Vps30/Atg6	BECN1	Component of PtdIns3K (complex I and II in yeast)
	Atg14	ATG14	Component of PtdIns3K (complex I in yeast)
Ubiquitin-like conjugation systems	Atg3	ATG3	E2-like enzyme for Atg8 conjugation
	Atg4	ATG4A to ATG4D	Cysteine proteinase
	Atg5	ATG5	Conjugated with Atg12
	Atg7	ATG7	E1-like enzyme
	Atg8	LC3A,B,B2,C, GABARAP,L1,L2	Ubl, conjugated to PE
	Atg10	ATG10	E2-like enzyme for Atg12 conjugation
	Atg12	ATG12	Ubl
	Atg16	ATG16L1,L2	Forms Atg12—Atg5–Atg16 complex

This table was modified from table 1 of Mizushima et al. (2011)

Table 1: The core molecular machinery of autophagosome formation[12].

ULK Complex

Mammals have two homologues of the yeast Atg1, ULK1 and ULK2, which are serine/threonine kinases that are largely functionally redundant for autophagy induction (ULK1 and ULK2 will be collectively be referred to as ULK hereafter)[13]. Atg13 binds to ULK and mediates the interaction of ULK and FIP200. Additionally, Atg13 binding stabilizes and activates ULK activity, leading to the phosphorylation of FIP200 by ULK. Atg101 associates with the ULK-Atg13-FIP200 complex, possibly via direct interaction with Atg13[14]. Atg101 recruits downstream factors to the phagophore[15]. Under basal conditions the mammalian target of rapamycin complex 1 (mTORC1)-mediated phosphorylation represses ULK activity[16]. However, nutrient starvation releases this inhibitory phosphorylation and upregulates ULK activity[17]. Activated ULK then phosphorylates several downstream components of the autophagy pathway, including pro-autophagic ATG14-containing VPS34 complexes[18–20]. Autophagic VPS34 complexes are recruited to the phagophore where they phosphorylate phosphatidylinositol (PtdIns) to produce phosphatidylinositol (3) phosphate (PtdIns (3) P)[21]. PtdIns (3) P functions as a platform bridging downstream components like the ATG16L1 complex to promote autophagosome formation. Additionally, mTORC1 has been shown to directly regulate the activity of VPS34 complexes, thereby allowing tight control of autophagy initiation in response to stresses[22]. Downstream of VPS34, ATG16L1 forms a trimeric complex with ATG5 and ATG12. ATG16L1 is the subunit responsible for recruiting the E3-like enzyme to the phagophore[1,23]. ATG12 acts to recruit microtubule-associated protein 1 light chain 3 (LC3) to the expanding autophagosomal membrane and ATG5 catalyzes the conjugation of the ubiquitin-like LC3 to

phosphatidylethanolamine in membranes of nascent autophagosomes, thereby driving their development[23,24]. Activation of autophagy can also be induced by changes in the cellular ATP-to-AMP ratio, where lower ratio indicates lack of cellular energy, which can be caused by conditions such as in glucose starvation[25]. AMP-activated protein kinase (AMPK) and STK11 (LKB1) serine/threonine-proteins kinases sense low cellular ATP levels and activate cellular processes in response to energy depletion[26]. Activation of autophagy via AMPK can occur through inhibition of mTORC1, either with indirect activation of TSC2 (tuberous sclerosis 2) complex by LKB, or directly through inhibitory phosphorylation of Raptor, both resulting in the inhibition of mTORC1[27]. AMPK can also activate autophagy by directly phosphorylating ULK1 at S317 and S777, VPS34 and Beclin 1[18].

Class III phosphatidylinositol 3-kinase complex (VPS34)

VPS34 is known to serve as a regulator of endosomal traffic to the Golgi and lysosomes; however, VPS34 has an important role in autophagy[28]. In mammals, the autophagy initiating VPS34 complexes consist of BECLIN-1, VPS15 and ATG14L are activated by cell stresses[29]. In contrast mammalian VPS34 complexes that regulate endocytic trafficking are inhibited during cell stress[30]. Another VPS34 complex containing UVRAG (UV irradiation resistance-associated gene, a putative homolog of yeast Vps38) has been shown to regulate VPS34 activity on late endosomes and on the mature autolysosome and is important for late-stage autophagy[31]. Rubicon (also known as KIAA0226) is a negative regulator of autophagy that competes with UVRAG for binding to the VPS34

complex[32]. VPS34 promotes the initiation and maturation of autophagosomes through the ATG14 and UVRAG-containing complexes, respectively[31].

Transmembrane Proteins

In mammals, the only two transmembrane proteins known to be required for autophagy are Mammalian Atg9 (mAtg9) and vacuole membrane protein 1 (VMP1)[11]. mATG9 is located in the late endosomes and the trans-Golgi network[33]. Under starvation or rapamycin treatment, it re-locates to the organelle periphery, where it overlaps with GFP-LC3-positive autophagosomes[34,35]. Regulation of mAtg9 upon starvation is ULK1-dependent, and also involves VPS34 activation, which is comparable to the yeast Atg9[29]. Through live cell imaging experiments, the formation of autophagosome was observed to be occur when ATG9 vesicles co-localize with the ER[36]. Mutation in Atg9 in both yeast and mammal led to failures of autophagosome formation, indicating that Atg9 may act to provide a lipid/membrane source for the autophagosome[36]. The transmembrane Vacuole-Membrane-Protein-1 (VMP1) does not have a homolog in yeast, but is also suspected to play a crucial role in the initiation of autophagy in higher eukaryotes[37]. The expression of VMP1 activates autophagy even upon nutrient-rich conditions[37]. In addition, autophagy is completely abolished in the absence of VMP1[38].

WIPI Protein Family

Human WIPI proteins are a part of the PROPPIN family proteins that functions as PtdIns (3) P effectors[39]. Both WIPI1 and WIPI2 are localized at the endosomes and nascent autophagosomes, which can specifically bind to PtdIns (3) P through conserved amino acids in their WIPI β-propeller sequences[40]. As discussed in the previous section, production of PtdIns (3) P by VPS34 on the ER has been shown to be a pre-requisite

leading up to phagophore formation from ER membrane[41]. WIPI proteins are recruited to the PtdIns(3)P on the phagophores and perform a fundamental effector function at the nascent autophagosome, as WIPI2 is reported to be directly responsible for recruitment of the downstream E3-like ATG16L complex to the phagophore for lipidation of LC3[42].

Two Ubiquitin-Like Proteins, Atg12 and Atg8/LC3, and Their Conjugation Systems

In mammals, two ubiquitin-like conjugation systems have been described to act in a core mechanism allowing elongation of the pre-autophagosomal membrane and formation of mature autophagosomes[43]. The formation of an isopeptide bond between ATG12 and ATG5 in the ATG12-ATG5-ATG16L1 complex is the product of the first conjugation system[44]. Ubiquitin-like protein ATG12 is conjugated to ATG5 through processing by the E1-like enzyme ATG7, and E2-like enzyme ATG10[43]. The interaction of ATG5–ATG12 with ATG16L1 leads to the formation of a trimeric complex at the membrane[16]. The second conjugation system includes Atg8-like proteins (yeast Atg8 has a number of human orthologues including LC3, GABARAP, and GATE-16)[45]. The conjugation of free LC3 (known as LC3-I) onto phosphoenthanoamine (PE) forming lipidated LC3 (known as LC3-II) by the E3-like ATG12-ATG5-ATG16L1 complex is one of the key markers of autophagosome formation[46]. LC3-II incorporation leads the elongation of the autophagosomal membrane, and LC3 also functions as docking sites for autophagic cargo adaptors[47]. This reaction is reversible, with LC3-II being able to be converted to LC3-I by the protease ATG4, making LC3 conjugation a key regulatory process of autophagosome biogenesis[48].

Selective Autophagy

Unlike bulk autophagy, selective autophagy targets specific cellular materials such as aggregated proteins, damaged organelles, and invading pathogens in order to maintain intracellular homeostasis[49]. Selective autophagy requires highly specific cargo recognition and sequestration, which is achieved through specialised autophagic cargo receptors, these cargo receptors are then recruited to the autophagosome by interactions with GABARAP/LC3 family proteins, which are anchored in the autophagosomal membrane through conjugation onto phospholipids [50] (Fig.2).

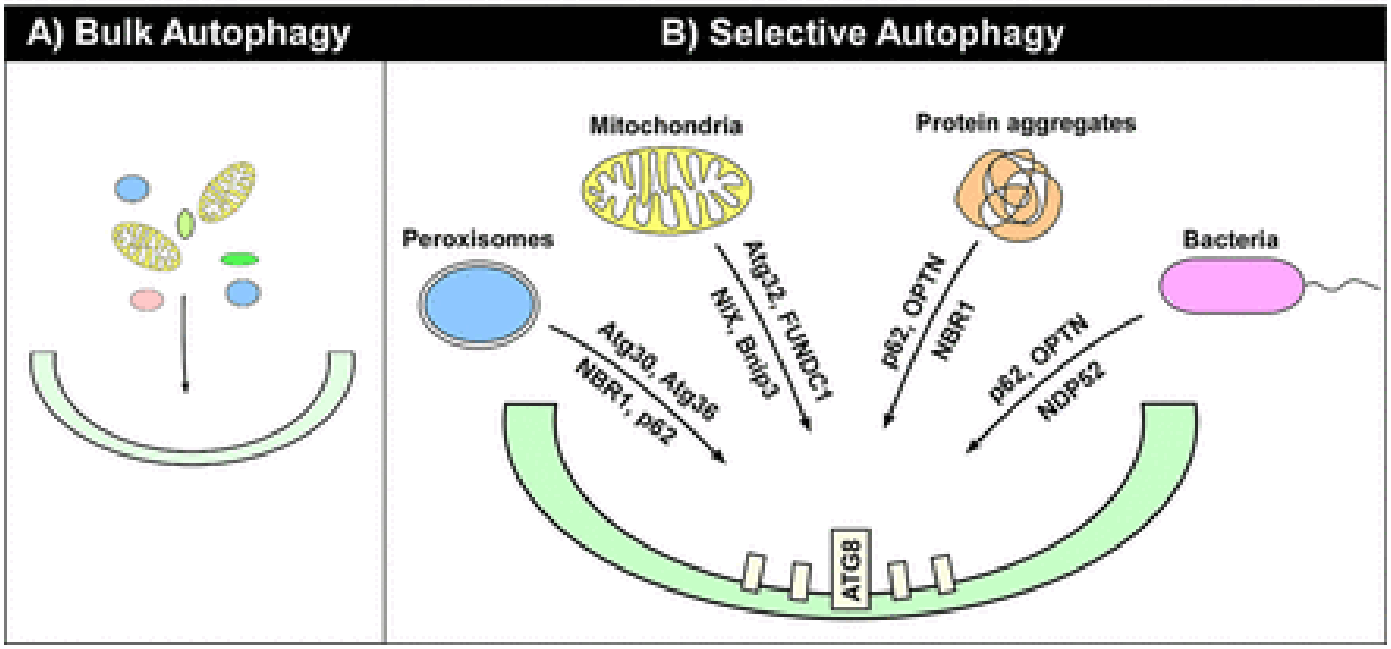

Figure 2: Bulk autophagy and selective autophagy[51]

Aggrephagy

Based on the nature of cargoes being degraded, selective autophagy can be classified into several subcategories[49]. Aggrephagy is the selective degradation of protein aggregates by autophagy[52]. Protein aggregates commonly arise from misfolded proteins as a result of mutations, incomplete translation, aberrant protein modifications or failing protein complex formations[52]. Protein misfolding exposes hydrophobic patches that can act as platforms for aggregate formation[51]. Together with unfolded protein response (UPR) aggrephagy serves the important function of protein quality control to eliminate misfolded proteins preventing the formation of aggregates from interfering with normal cellular functions[53]. Importantly, selective autophagy is essential for the degradation of large protein aggregates, since these types of large structures are likely inert to the UPR[52]. These aggregates are recognized by selective receptors of autophagy and recruited to the autophagosome[47]. In non-dividing cells such as neurons aggrephagy is especially important since the inability to clear such large aggregates lead to the irreplaceable loss of the cells[54]. Clearance of large protein aggregates occurs through the binding of the aggregate to the receptors that are recruited by ubiquitin on the protein aggregates[47]. These receptors in turn bind LC3 thereby allowing selective uptake of protein aggregates into autophagosomes[47]. The first identified selective autophagy receptor was the human protein p62/SQSTM1 (sequestosome 1), a scaffold protein that was known to involved in several essential signalling pathways[55]. It was also linked to a number of diseases that involved ubiquitin-containing protein aggregates, where p62 was found to accumulate in protein aggregation bodies[56]. This link to human pathophysiology

garnered more interest for selective autophagy as new focus of study in the autophagy field[56].

Xenophagy

Selective autophagy can also target invading pathogens, including intracellular bacteria, acting as a key component of the innate immune response[57]. Activation of anti-bacterial autophagy (hereafter referred to as xenophagy) involves the same key enzyme complexes in the autophagy pathway, but also requires xenophagy-specific proteins involved in pathogen-sensing that signal to the autophagy machinery during infection[58]. For instance, galectin-8 detects damaged *Salmonella*-containing vacuoles (SCV) and subsequently activates xenophagy through recruitment of the autophagy receptor NDP52[59]. Immunity related GTPase M (IRGM) has been shown to act as a scaffold bringing together ULK, Beclin-1-containing VPS34 complexes, and ATG16L1 to promote xenophagy initiation[60]. In addition to IRGM, ATG16L1-containing enzyme is also regulated by activation of intracellular (NOD2) sensors of bacterial peptidoglycan, where NOD2 binds ATG16L1 recruiting the LC3-lipidating enzyme to the site of bacterial infection[61].

Autophagy and Apoptosis

Autophagy and apoptosis can both occur in the same cell, usually with autophagy preceding apoptosis, since autophagy is activated by most stress signals, while the apoptotic pathway is only activated above a certain stress threshold[62]. Therefore, autophagy usually serves as a strategy for the cell to adapt and resist against stress[63]. On the contrary, apoptosis is a programmed suicide of cells and is executed by an array of proteases known as caspases. The caspases are activated through a proteolytic caspase cascade induced by a variety of both intra- and extracellular stress signals. Death receptors at cell surfaces or intracellular signals initiate the apoptotic process, signalling through a series of conserved cell death machinery proteins, leading to the cleavage of pro-caspases and their activation, promoting cleavage of further caspases in a cascade of caspases and also targeting a number of key cellular proteins, leading to the ultimate demise and removal of the cell in a highly ordered fashion[64].

When the cell commits toward the apoptotic fate, autophagy is inactivated, partially due to the apoptotic caspases targeting crucial autophagic proteins. Autophagy could also act to promote an apoptotic cell fate, by targeting critical components of the cell, facilitating the activation of apoptotic or necrotic programs, or just by proceeding at a rapid rate. The interplay between autophagy and apoptosis is complex, with cell fate highly dependent on the strength and duration initial stress signal[65].

Autophagy in Human Health and Disease

Over the past two decades autophagy research has become a rapidly expanding field. In particular, much enthusiasm has been directed toward understanding autophagy defects in disease. Autophagy defects have now been linked to multiple diseases including cancer, neurodegeneration, cardiovascular diseases and immune diseases[66].

Cancer

Defects in autophagy has long been observed in tumour cells. In 2003, Qu et al published their discovery of the first genetic link between an autophagy gene and cancer. They were able to demonstrate a high incidence of spontaneous tumours in beclin 1+/- mutant mice. When beclin 1 mRNA and protein expression of the tumour cells were analyzed, expression of wild-type beclin 1 transcript and protein were observed, indicating that beclin 1 was a haploinsufficent tumour suppressor. On the other hand, beclin 1-/- mice died early in embryogenesis and exhibited strongly altered autophagic response, establishing Beclin 1 as a key component of mammalian autophagic machinery. Together, these findings provided the earliest link between autophagy and cancer[67].

Neurodegenerative Disease

The aggregation of misfolded proteins and reduction of certain neuronal populations are some of the most established pathological events in neurodegenerative diseases[68]. As a crucial intracellular mechanism for removing proteins aggregates and damaged organelles, autophagy has been implicated in the pathological changes in several neurodegenerative diseases[69]. For example, Huntington's disease (HD) is a neurodegenerative disease caused by accumulation of the huntingtin protein (Htt), which

results in neuronal cell death with age[70]. A recent study indicates that the decrease in huntington protein aggregate burden by the drug CTEP (2-chloro-4-[2-[2,5-dimethyl1-[4-(trifluoromethoxy)phenyl]imidazol-4-yl]ethynyl]pyridine) correlated with the stimulation of autophagy regulated be the kinase GSK3β, the transcription factor ZBTB16, and the autophagy factor ATG14[71]. CTEP also inhibited the metabotropic glutamate receptor 5 (mGluR5) resulting in the activation of ULK kinase activity through inhibition of an inhibitory phosphorylation, increased the phosphorylation of ATG13, and increased level of Beclin1 in homozygous zQ175 mice[71]. These finding suggest that suppression of mGluR5 activity likely activates autophagy through multiple convergent pathways and leads to the clearance of mutant huntington protein aggregates, revealing a potential therapeutic target in HD patients[71].

Cardiovascular Diseases

Dysregulation of autophagy has been observed in diseases of the heart, including cardiomyopathies, cardiac hypertrophy, ischemic heart disease, and heart failure[72]. For example, temporally regulated cardiac-specific Atg5-deficient mice, result in left ventricular dilatation and contractile dysfunction, cardiac hypertrophy, along with increased levels of ubiquitination[73]. In addition, deficiency of Atg5 in the heart illustrated disturbed sarcomere structure and mitochondrial alignment and aggregation. These findings indicate that under baseline conditions, constitutive autophagy is fundamental for maintaining cardiomyocyte size, global cardiac structure and function in the heart[73]. In failing hearts, autophagy is upregulated as an adaptive response to ensure cells survival under hemodynamic stress[73].

Inflammatory Bowel Disease

Crohn's disease (CD) is a chronic inflammatory bowel disease typically affecting multiple separate segments of the gastrointestinal track, with a highly heterogeneous symptoms profile [74]. The disease onset can occur at any time point between early childhood to late adulthood[75]. Numerous studies have reported a disease prevalence of up to 1%, and suggest an increasing trend of new diagnosis in both developing and developed regions[76]. Despite its increasing prevalence, much of the etiology of CD remains unclear. Both genetic and environmental factors are believed to be involved in the development of this disorder[75]. An important identifying symptom of CD is the detection of granulomatous inflammatory response, where macrophages, epithelioid cells and multinucleated cells form inflammatory foci in the gastrointestinal wall[77]. It is believed to be caused by the presence of a long term stimulatory agent, and contributes to the development of necrosis and fibrosis[77]. The current model of Crohn's disease pathogenesis postulate that intestinal microbiota based stimulation in genetically pre-disposed individual leads to defective inflammatory responses, resulting in chronic inflammation of the gastrointestinal tract[78]. Therefore, understanding of the pathogen-host interactions and the complex network of signalling cascades involved would be key in search of new treatment options. Through genome-wide association studies (GWAS), researchers were able to identify high susceptibility regions of the genome that may be linked or contribute to the pathogenesis of CD, several of the proteins involved in xenophagy induction (ATG16L1 and IRGM) and pathogen detection (NOD2 and TLR4) were among the genes detected[79]. Interestingly, ATG16L1 and IRGM are not found in the related chronic inflammatory bowel disease ulcerative colitis (UC)[80]. GWAS have linked a non-synonymous single nucleotide

polymorphism (SNP) in ATG16L1 that substitutes threonine 300 for alanine with an increased susceptibility for CD[81]. Molecular characterization of the CD-associated ATG16L1 (caATG16L1) has shown that stresses such as starvation or pathogen infection enhance the susceptibility of caATG16L1 to caspase-mediated cleavage[61,82–84]. Enhanced cleavage of caATG16L1 has been shown to lead to an increase in inflammatory cytokine secretion and a decrease in xenophagy, which are thought to contribute to CD[61,85–87].

Another widely characterized signalling pathway involved in host inflammatory response is the NF-κB pathway. NF-κB is normally bound by the inhibitory IκB protein which blocks NF-κB from translocating to the nucleus. The pathway is activated through phosphorylation of IκB by an upstream IκB kinase complex (IKK), which consists of two catalytic subunits IKKα and IKKβ, and a regulatory IKKγ subunit. Interestingly, a recent study has found that IκB kinase subunit IKKα is capable of phosphorylating ATG16L1 on Serine 278 (S278), which regulates the sensitivity of caATG16L1 to caspase cleavage[85]. The caspase cleavage site on ATG16L1 lies in between the S278 phosphorylation site and the T300A Crohn's SNP. This raises the interesting possibility that phosphorylation of ATG16L1 in response to infection leads to inappropriate cleavage if the site is in close proximity to the T300A mutation. ATG16L1 contains several conserved serine/threonine residues proximal to T300, which may also be phosphorylated and may potentially regulate ATG16L1 function. However, it remains to be seen what effect phosphorylation has on wild-type ATG16L1 and if other stressors or kinases regulate ATG16L1 phosphorylation. In this study we hypothesize that ULK, the only protein kinase in the

autophagy pathway, phosphorylates ATG16L1 under starvation and infection, which may have important implications for Crohn's disease pathogenesis.

Material and Methods

Antibodies and Reagents

Anti-IKKα (Cat#2682), HA-HRP (#Cat 2999) and phospho-S6K T389 (Cat#9234) antibodies were obtained from Cell Signaling Technology. Anti-LC3B (Cat#PM036 for immunofluorescence) and ATG16L1 (Cat#PM040 for immunofluorescence) antibodies were purchased from MBL. Beta-Actin (Cat#A5441 clone AC-15) antibody was obtained from Sigma. DYKDDDDK Epitope Tag (Cat#NBP1-06712 for WB) antibody was purchased from Novus Biologicals. Anti-LPS FITC (Cat#sc-52223) and GST (Cat# sc-374171) antibodies was purchased from Santa Cruz Biotechnology. Anti-S6K (Cat#ab32529), LPS (Cat#ab128709), ATG16L1 (Cat#ab187671) antibodies were obtained from Abcam. phospho-ATG16L1 serine 278 was made in collaboration with Abcam. Polyclonal sera was affinity purified by phospho peptide and recombinant ATG16L1 (non-phosphorylated) was mixed in at a 6:1 molar ratio (Rec. ATG16L1: IgG), prior to immunoblotting. Monoclonal phospho-antibody from a hybridoma generated from this rabbit was used for immunofluorescence (Abcam Cat#ab195242). Active GST-ULK1 (1-649) and GST-ULK2 (1-478) from insect cells were purchased from CQuential Solutions (Moraga, CA). Anti-His-HRP (Cat#460707) was obtained from Invitrogen. Z-VAD(OMe)-FMK (Cat#HY-16658-1MG) was purchased from MedChemExpress. Bafilomycin A1 was obtained from Tocris (Cat#133410U). ULK-inhibitor MRT68921 was obtained from Selleckchem (Cat#S7949).

Cell Culture

MEFs, HEK293A, and HCT116 were cultured in DMEM supplemented with 10% Bovine Calf Serum (VWR Life Science Seradigm). IKKα wildtype and IKKα knockout cells were a generous gift from Dr. Michael Karin (University of California San Diego)31. ULK1/2 double knockout were a generous gift from Dr. Craig Thompson (Memorial Sloan Kettering)32. Amino acid starvation medium was prepared based on Gibco standard recipe omitting all amino acids and supplemented as above without addition of non-essential amino acids and substitution with dialyzed FBS (Invitrogen). Media was changed 1 hour before experiments.

Transfection

HEK293A cells were transfected with tagged ATG16L1 (750 ng) and tagged ULK1 (250 ng) using polyethylenimine (PEI, medistore uOttawa). HCT116 cells were transfected with the indicated tagged ATG16L1 (3-5 ug) using PEI.

1. Add 200ul of media without FBS into sterile Eppendorf tubes
2. Add planned tagged ATG16L1 (750 ng) and tagged ULK1 (250 ng) into the corresponding tubes
3. Add transfection reagent (PEI) (ratio: 4ul PEI to 1ug DNA) directly into the media containing DNA
4. Immediately after adding PEI, vortex to mix
5. Incubate DNA transfection mixture for ~15mins to 30mins to allow the formation of liposomes**.**

During the incubation, start to prepare the following cell suspension:

- Add 1ml Trypsin, incubate till the cells are lifted
- Add proper amount of media (with FBS) to dilute the confluency to around 20% per ml
- Transferring proper amount of the cell culture into a 15ml centrifuge tube
- Centrifuge at 1200rpm for 5 minutes
- Carefully remove the supernatant without touching the pellet
    a. Re-suspend the cell with 200ul per well of DMEM without FBS
- Add cell suspension to liposomes, pipette or invert the tube(s) once to mix

6. Incubate 5-10 minutes at room temperature.
7. After the incubation, add the mixture to destination wells containing complete media.
8. Media change on the next morning
9. The expression is transient, peak expression can be achieved at 36-48 hrs after transfection.

Generation of Stable Cell Lines

ATG16L1 knock-out lines were generated in the HCT116 background utilizing CRISPR/Cas9 targeting exon 1 (Fig. S3C). The knock-out HCT116 clones were infected with retrovirus carrying either wild-type or phospho-dead ATG16L1 at different amounts in order to achieve near endogenous levels of ATG16L1.

Cloning of ATG16L1 Mutations

Primer Design for ATG16L1 Mutations

length of PCR primers should be 18-22 bp, which is long enough for binding efficiency to the template at the annealing temperature.

- Primers used for **T300A mutation** are GGACAATGTGGATGCTCATCCTGGTTC (forward) and GAACCAGGATGAGCATCCACATTGTCC (reverse).
- Primers used for **S278A mutation** are GCCTTCTGGATGCTATCACTAATATC (forward) and GATATTAGTGATTGCATCCAGAAGGC (reverse).
- T300A followed by S278A mutation was performed to generate S278/T300A double mutation.

Site-directed Mutagenesis (SDM) of GST-HA ATG16L1 Mutations

- Site-directed mutagenesis (SDM) is a technique used to create one mutate or more bases in a plasmid. This method can change amino acid structure, damage transcription factor binding sites, or generate fusion proteins. SDM is usually used for explore the nucleic acids and proteins biological activity and structure, also SDM is can utilized for initiating or abolishing restriction enzyme recognition sites to facilitate cloning. In this study, site-directed mutagenesis was performed based on KOD Xtreme Hot Start DNA Polymerase kit instructions purchased from Thermo Fisher.

Cycling Conditions (PCR)

Thermocycling Steps

1. Polymerase activation	98 °C for 2 min
2. Denature	98 °C for 10 s
3. Annealing	64.5 °C for 30s
4. Extension	68 °C for 8 min
5. Repeat Steps 2-4	30 cycles

Transformation of GST-HA ATG16L1 Mutations

Bacterial transformation is technique used to produce multiple copies of DNA or gene of interest, which mostly in the form of a plasmid. The bacteria used in this transformation is DH5-Alpha Cells that were engineered from E. coli cells in order to increase transformation efficiency.

- Thaw competent DH5-Alpha Cells (50ul) on ice from -80°C for 10 min
- Gently re-suspend competent cells, by pipetting the cells once
- Add 1ug of GST-HA ATG16L1 T300A or S278A
- Place tubes on ice for 30 min
- Heat shock for 42°C for 90 seconds as appropriate for the bacterial strain and DNA used
- Place tubes on ice for 5 min
- Add 1000ul of Lysogeny broth (LB)
- Shake for 30 min at 37°C, 250rpm

- spend down the cells at 3000g for 1 min, remove majority suspension, leave about 100ul in the tube, then re-suspend cells by pipetting up and down gently beside the cell pellet
- plate the cells onto the plate with antibiotic (Carbomacylin)
- Grow Overnight at 37°C it should be between 16-18 hr

Next day, pick 10 single colonies and put into the 4ml of LB culture with Carbomacylin, then shake it overnight at 37°C, 250 rpm

After growing the bacteria in LB overnight we used mini-preparation (miniprep) of plasmid DNA, which allows the isolation of plasmid DNA from bacteria. The miniprep kit instructions purchased from Bio Basic. The extracted plasmid DNA from DH5-alpha bacteria was measured by using a Nanodrop-1000.

Stable cell line expressing the Mutations generation/ characterization

The epithelial intestinal HCT116 cells were selected because they are commonly used to study ATG16L1-mediated xenophagy. The knock-out HCT116 clones were infected with retrovirus carrying either wild-type or phospho-dead ATG16L1 at different amounts in order to achieve near endogenous levels of ATG16L1.

For GST- HA ATG16L1 virus production and purification:

1. Starting the production by using HEK293A cells at 30% confluence for 10 cm plate
2. Transfect 3ug GST-HA ATG16L1, 1ug pPAX2, 0.25UG VSV-G with a 1:4 DNA: PEI ratio

3. Media change after 5 hr of the transfection
4. Next day, start collecting the media and store at 4°C, then add 5ml media
5. Repeat step 4 every 12 hr for 4 days.
6. At the last time of collecting GST-HA ATG16L1, cells were lysed using 1X SB and run SDS-Gel to observe transfection efficiency by blotting GST or HA
7. Then, using the virus precipitation kit instructions obtained from Benchmark bioscience, in order to purified the virus carrying the plasmid of interest

Infection of GST-HA ATG16L1 Carrying Mutations and Puromycin Selection

The ATG16L1 knock-out clones were infected with viruses carrying either wild-type, or phospho-dead ATG16L1 at different amounts (10, 50,100ul) in order to achieve near endogenous levels of exogenous ATG16L1.

Cells were treated with Puromycin (2ug) for 3 days, and sent for sequencing after recovery.

Bacterial Strains

Wild-type (SL1344) *Salmonella* was a gift from Dr. Subash Sad, (University of Ottawa). Bacteria were grown in Luria-Bertani broth (Fisher).

Bacterial Infection

Salmonella were grown in 4 mL of LB broth at 37 degrees Celsius at 250 rpm. Overnight cultures of *Salmonella* were diluted 30-fold and grown until OD_{600} reached 1.5, followed by centrifugation of 10,000 g for 2 min, and resuspension in 1 mL of PBS. Bacterial stock

was then diluted 5-fold (MOI = 900) in DMEM supplied with 10% heat-inactivated Bovine Calf Serum for infection. Cells cultured in antibiotic-free medium were infected with *Salmonella* and incubated at 37 degrees Celsius in 5% CO_2 for the indicated time. Cells were washed in PBS once before direct lysis with 1X denaturing SDS sample buffer.

Western Blot and Immunoprecipitation

Whole cell lysates were prepared by direct lysis with 1X SDS sample buffer. Samples were boiled for 10 min at 95 degrees Celsius and then resolved by SDS-PAGE on 6%-18% gradient polyacrylamide gels. SDS-PAGE was performed, and proteins were transferred to PVDF membrane then incubated for 20 minutes with blocking buffer (3% BSA or 5% skim milk in TBS-T), washed with TBS-T five times every 5 min and incubated with primary antibodies (1:1000 5% BSA in TBS-T) overnight at 4^{o}C. Next, membranes were incubated in appropriate horseradish peroxidase-conjugated secondary antibody (1:10000 in TBS-T 2% BSA or skim milk) for one hour at room temperature. Immune complexes were harvested from cells lysed in mild lysis buffer [10mM Tris pH 7.5, 10 mM EDTA, 100 mM NaCl, 50 mM NaF, 1% NP-40, supplemented simultaneously with protease and phosphatase inhibitor cocktails –EDTA (APExBIO)], followed by centrifugation at max speed for 10 minutes to remove cell debris. Protein A beads (Repligen) were washed 1X with PBS and incubated with antibodies and cell lysates for 1.5-3 hours followed by one 5-minute wash with MLB and inhibitors and 4 quick washes with MLB alone. Beads were boiled in 1X denaturing sample buffer for 10 min before resolving by SDS-PAGE.

Immunofluorescence

Cells were plated on IBDI-treated coverslips overnight. After treatments, cells were fixed by 4% paraformaldehyde in PBS for 15 min and subsequently permeabilized with 50 µg/mL digitonin in PBS for 10 min at room temperature. Cells were blocked in blocking buffer (1% BSA and 2% serum in PBS) for 30 min, followed by incubation with primary antibodies in the same buffer for one hour at room temperature. Samples were then washed 2X in PBS and 1X in blocking buffer before incubation with secondary antibodies one hour at room temperature. Slides were washed 3X in PBS, stained with DAPI, and mounted. Images were captured with inverted epifluorescent Zeiss AxioObserver.Z1. In the case of outside/inside bacterial staining, before permeabilization, the cells were incubated with anti-LPS antibody and corresponding secondary antibody in blocking buffer, accompanied by 3X PBS washes in between.

Quantification of Immunofluorescence

An automated protocol built in the Image J software was used to analyse epifluorescent microscopy images to avoid bias. The same protocol was applied to each field of view and across samples. An average of 8 unique fields of view from representative experiments were selected for quantification.

in vitro ULK Kinase Assay

HEK293A transiently expressing tagged ATG16L1 were immunoprecipitated. Pulldown proteins were washed 3X with MLB and 1X with MOPS buffer and were used as substrates for ULK kinase assay. ULK proteins were immunoprecipitated and extensively washed with MLB (once) and RIPA buffer (50 mM Tris at pH 7.5, 150 mM NaCl, 50 mM NaF, 1 mM EDTA, 1 mM EGTA, 1% SDS, 1% Triton X-100 and 0.5% deoxycholate) once,

followed by washing with MLB buffer once followed by equilibration with ULK1 assay buffer (kinase base buffer supplemented with 0.05 mM DTT, 10 µM cold ATP, and 0.4 µCil 32P-ATP per reaction). Reactions were shaken at 250 rpm at 37 degrees Celsius for 30 min and stopped by direct addition of 4X sample buffer followed by 10 min boiling at 95 degrees Celsius and resolution by SDS-PAGE. The analysis of kinase reactions necessitated the separation of the kinase and substrate. In vitro kinase reactions were analyzed by autoradiograms.

Mass Spectrometry

A gel band corresponding to the ATG16L1-GST fusion protein was cut from a SDS–PAGE gel after an in vitro kinase reaction. The gel band was subjected to in-gel trypsin digestion and the resulting peptide mixture was subjected to liquid chromatography coupled to tandem mass spectrometry. Protein and modification identification was performed with the database search algorithm X!Tandem and peptide identifications were validated with Peptide Prophet.

Colony Forming Unit (CFU) Assay

Cells were infected with *Salmonella* (MOI of 180) for 1 hour. The infected cells were washed 2X and incubated with media containing 100 µg/mL Gentamicin for 0.5 hour, followed by 4-hour incubation with media containing 50 µg/mL Gentamicin. The samples were rinsed 3X with PBS and lysed with CFU buffer (0.1% Triton X-100 and 0.01% SDS in PBS). The harvested lysates were serially diluted (1:100, 1:300, and 1:1000) and plated onto LB agar plates containing Streptomycin. The plates were incubated at 37 degrees Celsius for 16-18 hours and the colonies were counted to determine the number of CFU.

Statistical Analysis

Error bars for Western blot analysis represent the standard deviation between densitometry data collected from 3 unique biological experiments. Statistical significance was determined using paired Student's one-tailed T-test for two data sets.

*Unless otherwise indicated experiments were performed three times. Data are represented as mean ± standard deviation and p values. were determined by Student's T-Test.

Results

ATG16L1 Is Phosphorylated by ULK

Starvation has been described to trigger caspase-mediated cleavage of ATG16L1 containing a common amino acid substitution (T300A)[21]. A recent study has established that IκB kinase subunit IKKα phosphorylates ATG16L1 on Serine 278 (S278), which promotes caATG16L1 to caspase cleavage[85]. However, IKKα has not been implicated in starvation-induced autophagy. Interestingly, ATG16L1 has been shown to bind FIP200, an essential co-factor of the ULK1 kinase complex. The interaction of ATG16L1 with FIP200 has been shown to be involved in regulating ATG16L1 localization in autophagy induction[27,28]. Therefore, we hypothesized that ULK1/2, the only protein kinases in the autophagy pathway, may phosphorylate ATG16L1 under starvation. To test this hypothesis, we performed an *in vitro* kinase assay using either purified ULK1 or ULK2 with recombinant ATG16L1 as substrate. We found that both ULK1 and ULK2 were capable of phosphorylating ATG16L1 *in vitro* (Fig. 3A). In order to narrow down the site of phosphorylation we repeated the kinase assay using truncations of ATG16L1. We found that the truncation mutant lacking amino acids 254-294 was a very poor substrate for ULK1, indicating that the primary site(s) of ULK1-mediated phosphorylation are located in this region (Fig.3B).

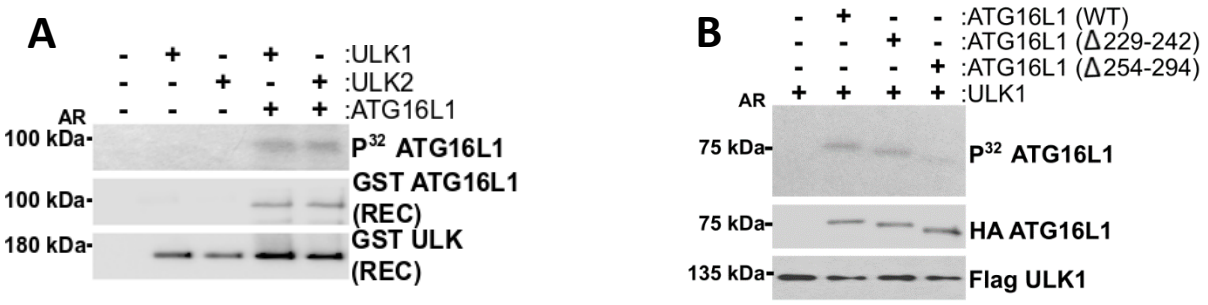

Figure 3: ULK kinases phosphorylate ATG16L1. (A) In vitro kinase assays were performed using purified recombinant kinases (ULK1 and ULK2) and substrate (ATG16L1) in the presence of radiolabelled ATP. ULK and ATG16L1 inputs were examined by western blot (WB) and substrate phosphorylation was analyzed by autoradiography (AR). **(B)** Full-length or truncated versions of ATG16L1 were subjected to an in vitro ULK1 kinase assay. ULK1 and ATG16L1 inputs were examined by western blot and target phosphorylation by autoradiography

Amino acids 254-294 are serine/threonine rich, containing 10 conserved residues (Fig. 4). Therefore, to identify the residue(s) that are phosphorylated by ULK1 in this region we repeated the kinase assay on full length ATG16L1 and performed mass spectrometry analysis. Our results revealed a single high confidence phosphorylation site on serine 278 (Fig. 4B and marked in green in Fig. 4A) and another of slightly lower confidence on serine 287 (Fig. 4B and marked in grey in Fig. 4A), both of which map to the region of ATG16L1 we previously identified as required for ULK1-mediated phosphorylation (Fig. 3). Peptide coverage in the mass spectrometry was 80% across the whole protein and only two S/T residues were missed in the putative 254-294 region. To confirm the major site(s) of phosphorylation on ATG16L1 we mutated S278 and S287 singly in the full length protein and performed another in vitro ULK1 kinase assay.

A

B

pS287

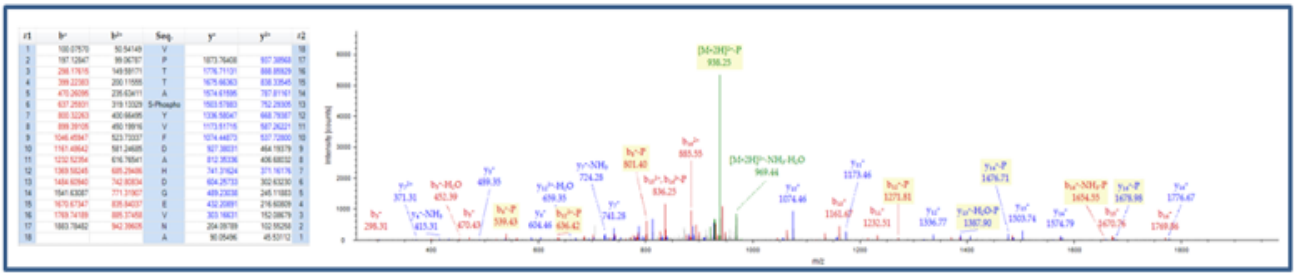

pS278

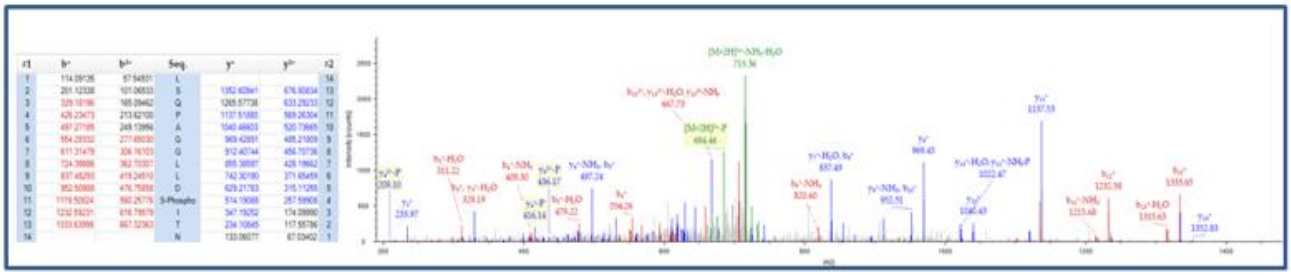

Figure 4: ULK phosphorylates ATG16L1 on S278. (A) ATG16L1 was phosphorylated in an in vitro ULK kinase reaction and analysed by mass spectrometry. Phosphorylation of S278 and S287 in human (S278 marked in green, S287 marked in grey) was identified with high and low confidence, respectively. Conservation of amino acids 254-294 are shown using the Shapely colour scheme. Mass spectrometry was performed on a single experiment. **(B)** Mass spectrometry data for ULK-mediated ATG16L1 phosphorylation.

Interestingly, we observed a significant loss of ULK1-mediated phosphorylation in the S278A mutant and little reduction in the S287A mutant (Fig. 5A). This indicates that the major site of phosphorylation on ATG16L1 is S278, which is the same residue previously identified as a site for IKKα mediated phosphorylation[24]. Next, we created phospho-specific antibodies against S278 or S287 of ATG16L1 and tested its specificity by co-transfection of wild-type or mutant ULK1 and ATG16L1. Excitingly, we observed that ULK1 phosphorylates ATG16L1 on S278 in cells and that our antibody was specific to the phosphorylated form of the protein with little to no signal against ATG16L1 (S278A) or wild-type ATG16L1 co-transfected with kinase-dead ULK1 (Fig. 5B). Despite good specificity for our S287 antibody (Fig. 5C, 5D) we observed that the lower probability site obtained by mass spectrometry, S287, was not phosphorylated in an ULK1-dependent manner (Fig. 5B). Collectively, these results show that ATG16L1 is a direct target of ULK1 and that the primary site of phosphorylation is S278.

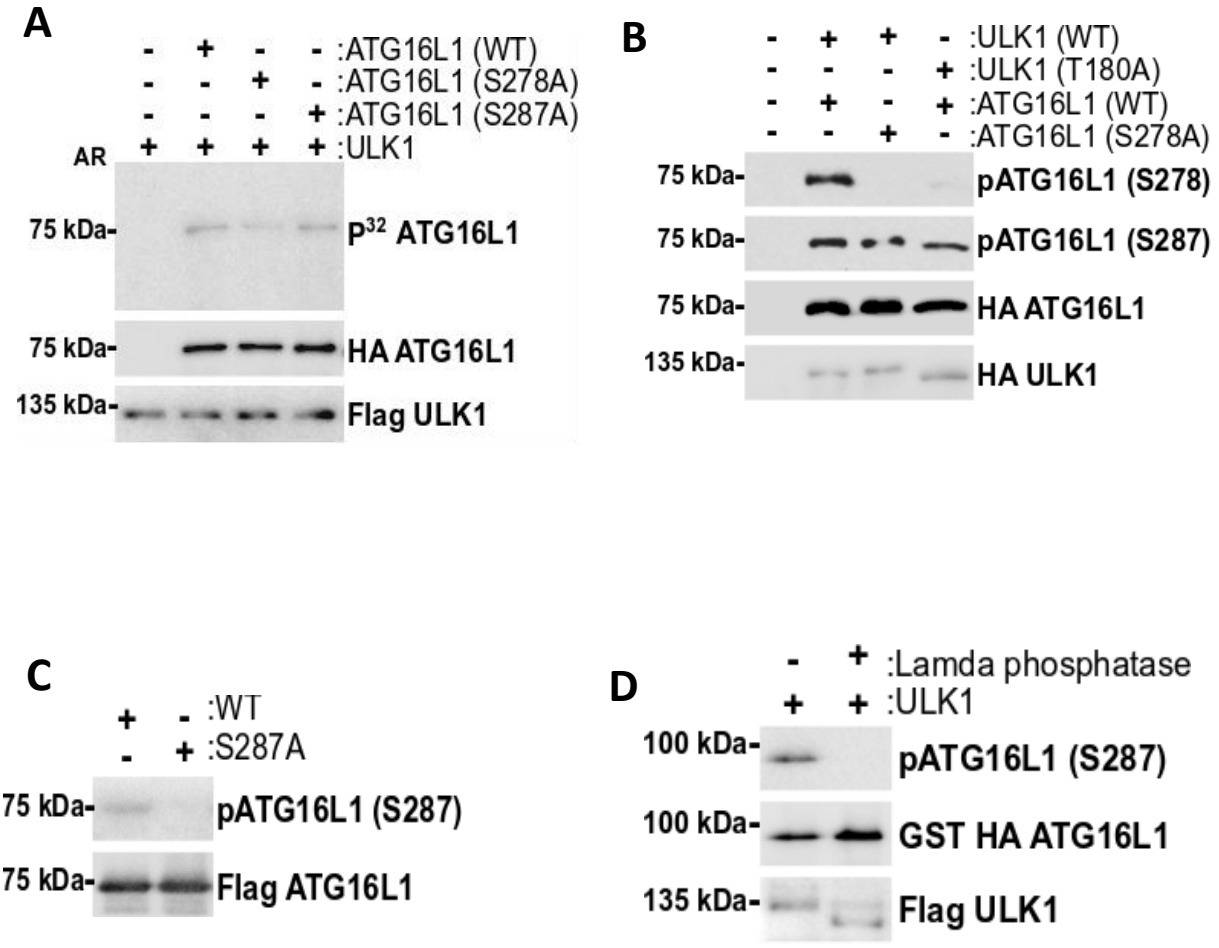

Figure 5: ULK phosphorylates ATG16L1 on the S278. (A) Full-length or mutated HA-ATG16L1 was purified from mammalian cells and subjected to an in vitro ULK1 kinase assay. Inputs were analysed by WB and target phosphorylation by AR**. (B)** HEK293A cells were transfected with wild-type or phospho-dead ATG16L1 in the presence of wild-type or kinase-dead ULK. Phosphorylation of ATG16L1 (S278 or S287) and inputs were examined by WB**. (C)** ATG16L1 knock-out HEK293A were transfected with either flag-tagged wild-type or S287A ATG16L1. Phosphorylation of ATG16L1 at S287 was determined by WB. **(D)** Wild-type ATG16L1 substrate and ULK1 were incubated with or without lamda phosphatase. Phospho-specificity of ATG16L1(S287) antibody was determined by immunoblot for total- and phospho-ATG16L1

ULK1 is required for phosphorylation of ATG16L1 and xenophagy induction

We next sought to determine if ULK1 regulated ATG16L1 phosphorylation endogenously and whether this signalling was responsive to starvation. ULK1/2 wild-type or ULK1/2 double knockout (dKO) cells were starved for amino acids, either with amino acid-free DMEM or HBSS, followed by analysis of pATG16L1 levels by western blot of whole cell extracts. Starvation potently inhibits mTORC1-signalling, as demonstrated by loss of S6K phosphorylation, which is a prerequisite for ULK1 activation. Importantly, we observed that starvation resulted in a clear increase in endogenous ATG16L1 phosphorylation only in cells containing ULK1 (Fig. 6A, lanes 1-6). Notably, our phospho-antibody only recognizes the slower migrating ATG16L1β isoform and is observed as a single band. As IKKα was previously described to phosphorylate ATG16L1 on S278 under infection we also tested the requirement for IKKα in starvation-induced ATG16L1 phosphorylation. However, we observed that IKKα-deficiency had no detectable effect on starvation-induced ATG16L1 phosphorylation (Fig. 6A, lanes 7-9). We found that ablation of ULK1-mediated phosphorylation of ATG16L1 had no effect on the stability of the ATG16L1/5-12 complex (Fig. 6B).

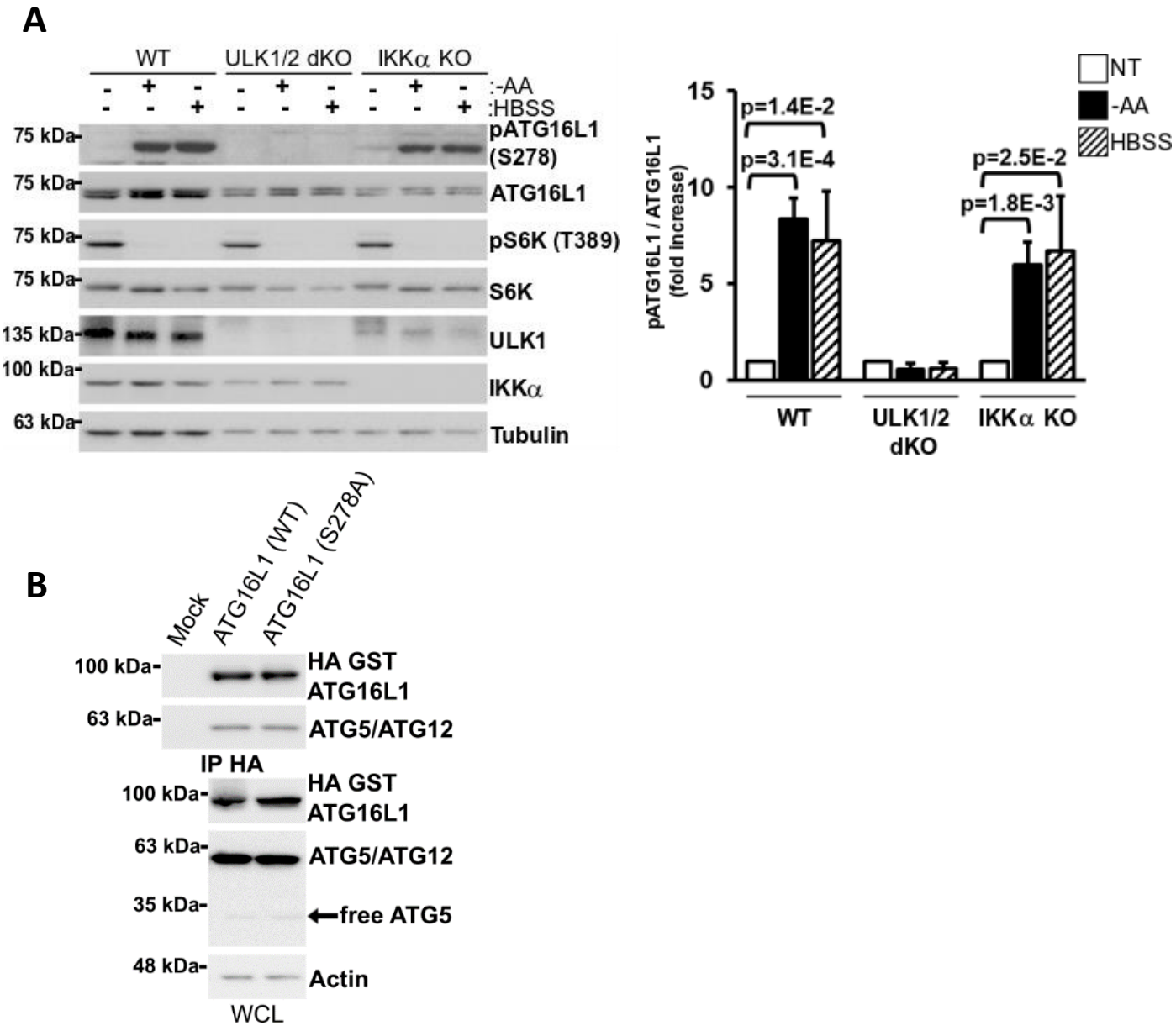

Figure 6: ULK, not IKKα, phosphorylates ATG16L1 on S278 in response to starvation. **(A)** Wild-type, ULK double knockout (dKO), or IKKα KO mouse embryonic fibroblasts (MEFs) were incubated with either complete medium, amino acid-deficient DMEM, or HBSS for 1 hour. Samples were immunoblotted using the indicated antibodies. **(B)** ATG16L1 knock-out HEK293A transfected with the indicated GST HA ATG16L1 plasmids were immunoprecipitated for HA. WB was used to examine the binding of ATG5/ATG12 to ATG16L1.

This is perhaps expected as IKKα has no known role in starvation-induced autophagy. This result indicates that the ATG16L1 subunit of the LC3-lipidating enzyme is a direct and physiological target of ULK1 under starvation. We next asked if ULK1/2 or IKKα contributed to ATG16L1 phosphorylation upon infection or TNFα treatment. ULK1/2 wild-type, ULK1/2 dKO, or IKKα KO were infected with *Salmonella* enterica serovar Typhimurium (hereafter referred to as *Salmonella*) or treated with TNFα and ATG16L1 phosphorylation was examined by western blot. Surprisingly, we observed that *Salmonella* and TNFα-induced ATG16L1 phosphorylation was abolished in ULK1/2 dKO cells, but was still observed in IKKα knockout cells (Fig. 7A, 7B). Of note, phospho-ATG16L1 signal is consistently lower under infection as only a small minority of cells are subjected to the stress of internalized bacteria (Fig. 7C). These results clearly indicate that ULK1/2 is required for phosphorylation of ATG16L1 under starvation, inflammatory cytokine signaling and infection.

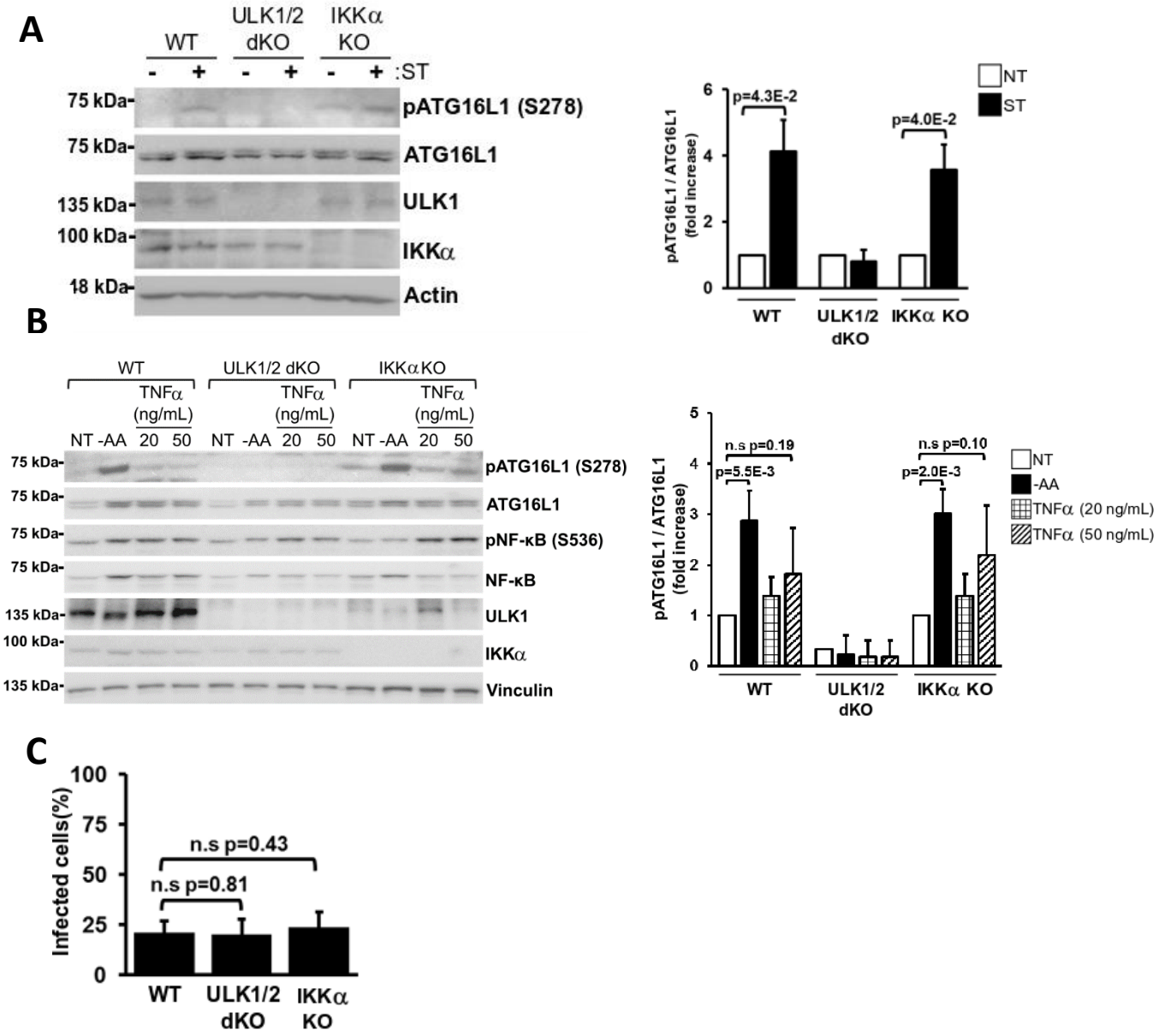

Figure 7: ULK, not IKKα, phosphorylates ATG16L1 on S278 in response inflammatory cytokine signaling and infection. **(A)** Wild-type, ULK dKO, or IKKα KO MEFs were infected with log phase *Salmonella* for 2 hours; bacteria-containing media was then removed and cells were incubated with gentamycin (50μg/mL)-containing DMEM for 2 hours. **(B)** Wild-type, ULK1/2 dKO, or IKKα KO MEFs were treated with either amino acid-free media or the indicated amounts of TNFα for 3 hours. Samples were immunoblotted using the indicated antibodies. Samples were immunoblotted using the indicated antibodies. **(C)** Wild-type, ULK1/2 dKO and IKKα KO MEFs were infected with *Salmonella* for 1 hour. Quantification of infected cells were examined through immunofluorescence**.**

We next sought to determine the requirement for ULK1/2 and IKKα in promoting xenophagy. Xenophagic clearance of *Salmonella* is very well established and its intracellular growth is restricted by the pathway, making it an ideal model pathogen for this analysis. Wild-type or knockout cells were infected with *Salmonella* and the number of LC3B-positive *Salmonella* were quantified. LC3B is conjugated to the autophagosomal membrane and colocalizes with bacteria targeted for clearance by xenophagy and can be used at early time points to monitor xenophagy induction. We found that ULK1/2-deficient cells exhibited a potent decrease in LC3B-positive bacteria, while IKKα loss did not significantly affect xenophagy (Fig. 8).

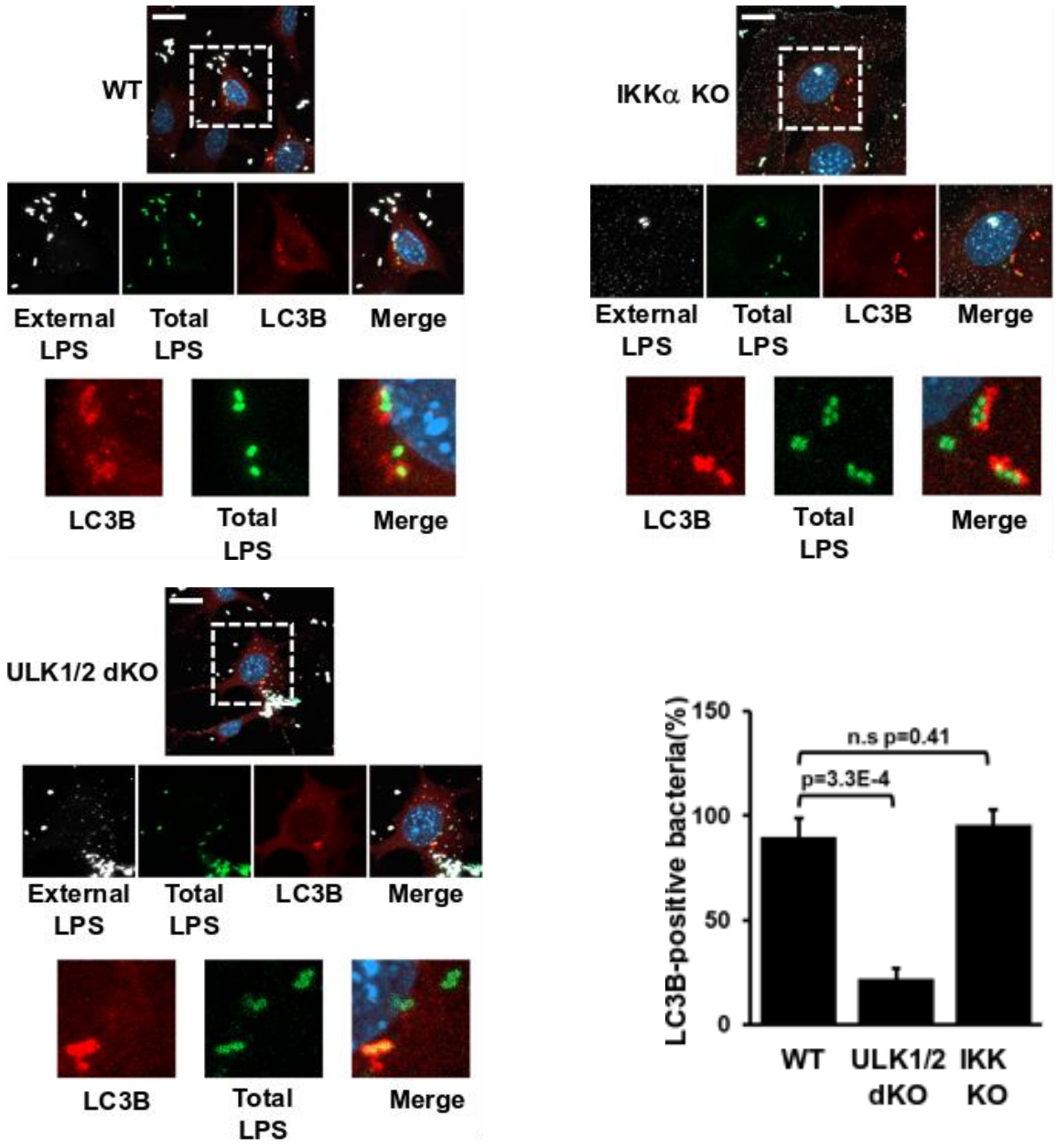

Figure 8: ULK, not IKKα, promotes xenophagy. Wild-type, ULK dKO, or IKKα KO MEFs cells were infected with *Salmonella* for 1 hour in the presence of Bafilomycin A1. Bacteria were stained using anti-LPS antibodies to analyze localization in addition to the autophagy marker LC3B. Representative immunofluorescent images of LC3B and LPS are shown (scale bars 20μm, 10μm). Quantification of bacteria undergoing autophagic clearance from 8 fields of view from a representative experiment is shown.

In order to confirm the roles for ULK1/2 and IKKα in xenophagy induction and suppression of invasive bacteria we performed colony forming unit (CFU) assays in our wild-type or knockout lines. CFU assays measure bacterial viability after internalization and are inversely correlated with xenophagy rates[29]. Analysis of *Salmonella* viability 4 hours post infection revealed that ULK1/2 dKO cells harboured a much higher number of viable internalized bacteria, indicative of an autophagy defect, when compared to wild-type and IKKα knockout cells (Fig.9). Surprisingly, our results indicate that ULK1/2, but not IKKα, is required for ATG16L1 phosphorylation and xenophagy induction.

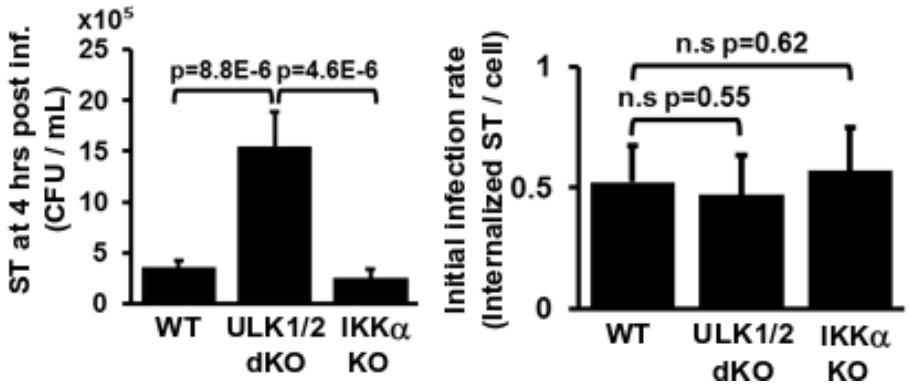

Figure 9: ULK, not IKKα, promotes bacterial clearance. Wild-type, ULK dKO and IKKα KO MEFs were infected with Salmonella for 1 hour. Xenophagy rates were examined through Colony Forming Unit (CFU) assays. Quantification of infection rates by immunofluorescence is demonstrated in the right panel.

ULK promotes cleavage of caATG16L1 through phosphorylation on S278

Multiple groups have shown that the T300A substitution in caATG16L1 renders it sensitive to caspase cleavage under stress conditions including nutrient starvation and infection[21,24,30]. Moreover, it was shown that mutation of serine 278 of ATG16L1 to alanine is involved in stress-induced caspase cleavage in the caATG16L1 background[24]. Our data indicate that ULK1 is responsible for the phosphorylation of wild-type ATG16L1 on S278 under nutrient starvation and infection. Therefore, we next sought to determine if ULK1 signalling was involved in the stress-induced destabilization of caATG16L1. HEK293A cells were transfected with either wild-type ATG16L1 or caATG16L1 co-transfected with increasing amounts of ULK1 kinase. Importantly, overexpression of ULK1 is known to result in autoactivation and induction of downstream signalling in the absence of stress, thereby allowing us to determine the isolated effect of ULK1 signalling on ATG16L1 stability independent of other stress-responsive pathways. Interestingly, we observed that ULK1 is capable of stimulating ATG16L1 cleavage and the level of cleavage is elevated in the caATG16L1 background (Fig. 10).

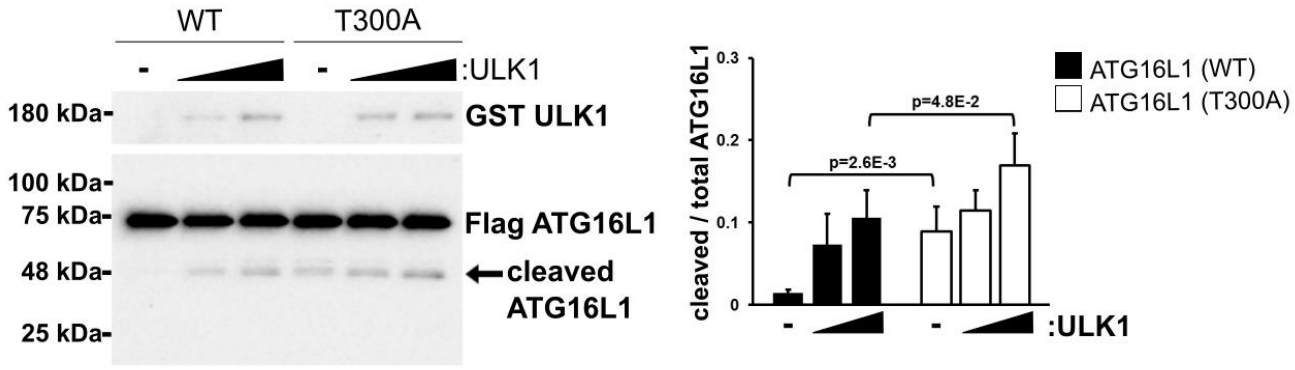

Figure 10: ULK induces caATG16L1 cleavage. HEK293A cells were transfected with either tagged WT-ATG16L1 or caATG16L1. ULK1 was co-transfected in increasing amounts where indicated. Cleavage of ATG16L1 was analyzed by WB of whole cell lysates. Levels of ATG16L1 cleavage are from 3 biological repeats (right panel, error bars denote S.D).

In order to determine if ATG16L1 cleavage was a result of ULK1-mediated phosphorylation on S278 we transfected HEK293A cells with wild-type, T300A, or S278/T300A mutants of ATG16L1 in the presence or absence of ULK1. Excitingly, we observed that single mutation of the ULK1 phosphorylation site was sufficient to reduce ULK1-driven cleavage (Fig. 11A). As expected mutation of S287, the low confidence ULK1 phosphorylation site identified by mass spectrometry, had no impact on cleavage in the T300A background (Fig. 11B). These results indicate that caATG16L1 is preferentially cleaved through ULK1-mediated phosphorylation of S278. Conversely, we found that T300A did not have any effect on ATG16L1 phosphorylation (Fig. 11C). Lastly, we repeated this experiment in the presence or absence of Z-VAD-FMK, a pan-caspase inhibitor, to confirm the faster migrating form of ATG16L1 was indeed a product of caspase-mediated cleavage. Treatment with a pan-caspase inhibitor resulted in a potent

reduction in the levels of the faster migrating ATG16L1 band, confirming that the ULK1-driven cleavage product was a caspase cleavage product (Fig. 11D).

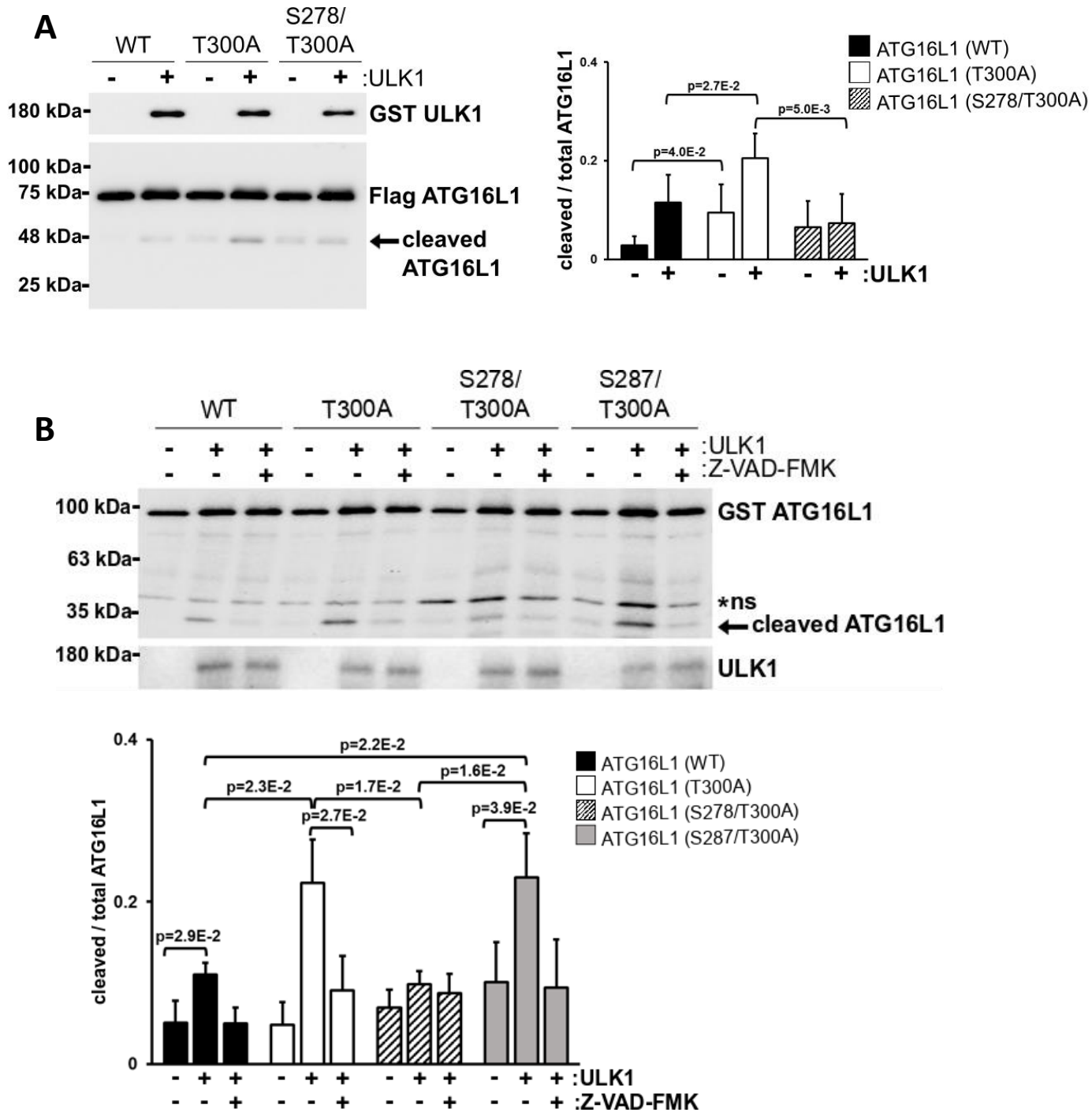

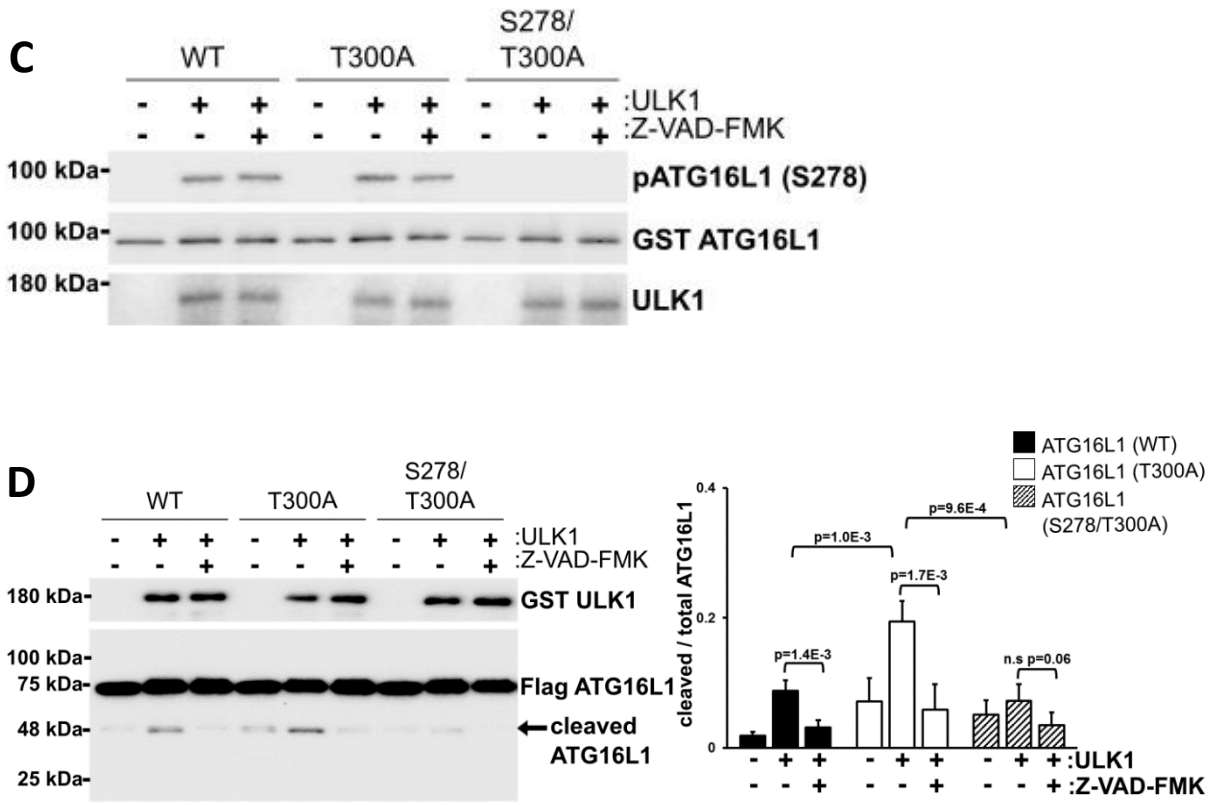

Figure 11: ULK-mediated ATG16L1 phosphorylation induces caATG16L1 cleavage.

(A) HEK293A cells were transfected with either tagged wild-type, S278A, or S278/T300A ATG16L1 in the presence or absence of ULK. **(B)** ATG16L1 knock-out HEK293A were transfected with the indicated GST HA ATG16L1 plasmids in the presence or absence of Z-VAD-FMK (15 µM) for 4 hours. Cleavage of ATG16L1 was analyzed by WB. **(C)** ATG16L1 knock-out HEK293A were transfected with the indicated GST HA ATG16L1 plasmids in the presence or absence of Z-VAD-FMK (15 µM) for 4 hours. Phosphorylation of ATG16l1 was analyzed by WB Cleavage of ATG16L1 was analyzed by WB. Levels of ATG16L1 cleavage are from 3 biological repeats (right panel, error bars denote S.D). **(D)** HEK293A cells were transfected with the indicated plasmids in the presence or absence of Z-VAD-FMK (15 µM) for 4 hours. Cleavage of ATG16L1 was analyzed by WB. A representative experiment of three repeats is shown. * denotes a p-value <0.05 as determined by Student's T-Test

Increasing evidence in vitro and in vivo has shown that caspase-mediated destabilization of caATG16L1 is a critical event associated with the pathobiology of this SNP[21,24]. Moreover, in unstressed conditions caATG16L1 is known to have the same stability as wildtype[21]. In order to determine the role of ULK1-signaling on T300A we transfected ATG16L1(T300A) in HEK293A cells and infected cells in the presence or absence of ULK-inhibitor. Interestingly we observed *Salmonella* treatment destabilized the T300A mutant, which could be reversed with ULK-inhibitor (Fig. 12A). However, ATG16L1(WT) stability was not drastically affected by either *Salmonella* or ULK-inhibition (Fig. 12A). We also found ATG16L1(T300A) was stabilized by ULK-inhibitors under TNFα treatment (Fig. 12B). We next sought to determine the function of S278 phosphorylation of ATG16L1 in both the wildtype and T300A background.

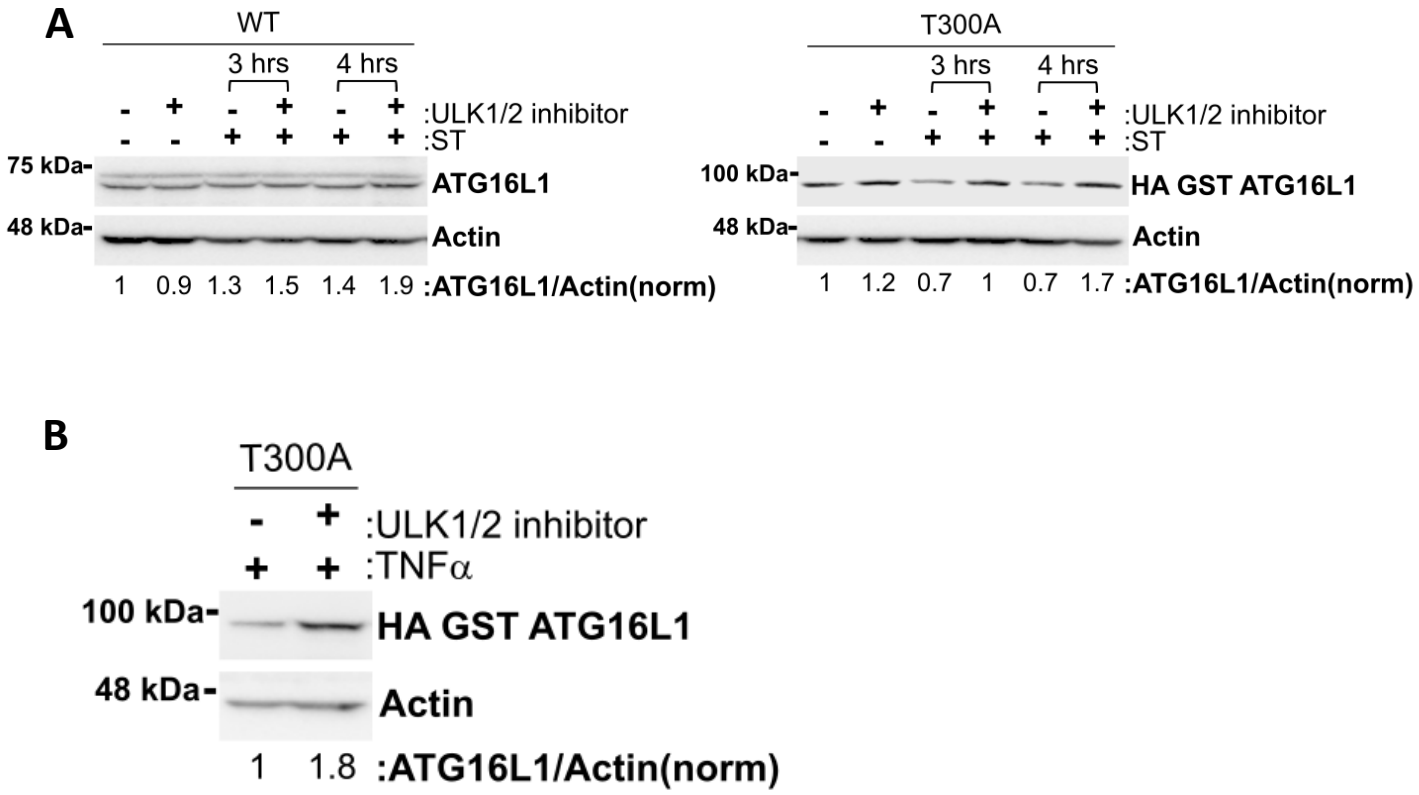

Figure 12: ULK dependent phosphorylation of ATG16L1 leads to estabilization of caATG16L1 but not in WT ATG16L1. **(A)** Wild-type or T300A-expressing HEK293A were treated with *Salmonella* in the presence or absence of ULK1/2 inhibitor (16 μM) for the indicated time points. Expression of ATG16L1 was analysed by WB. The experiments were performed twice. **(B)** ATG16L1 knock-out HCT116 transfected with the tagged T300A ATG16L1 plasmids were treated with TNFα (20 ng/mL) in the presence or absence of ULK1/2 inhibitor for 4 hours. ATG16L1 levels were examined by WB.

ATG16L1 knockout cells were transfected ATG16L1 (WT, S278A, T300A, or S278A/T300A) at similar levels (Fig. 13A) and were treated with Salmonella. Quantification of *Salmonella* at 4 hours post infection showed that mutation of S278 phosphorylation in the wild type background resulted in an increase in Salmonella, indicating ULK1 phosphorylation may act to promote xenophagy in wild-type ATG16L1 (Fig. 13B, column 1 and 2). Conversely, in the T300A background S278A mutation improved *Salmonella* clearance, indicating ULK1 phosphorylation is detrimental in this background (Fig. 13B, column 3 and 4).

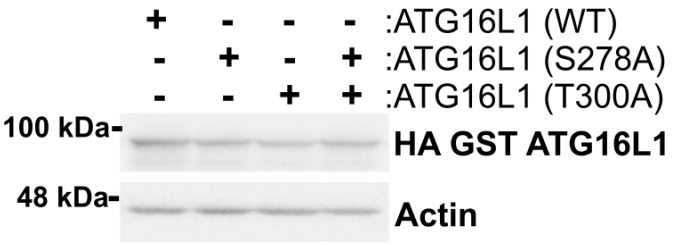

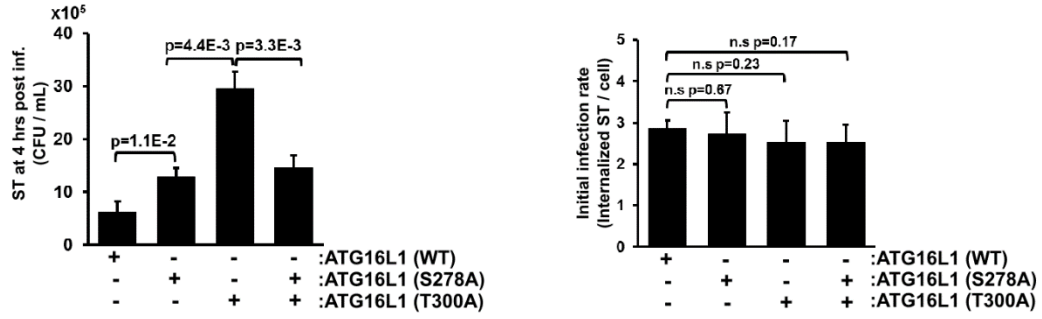

Figure 13 :ATG16L1 phosphorylation is required for bacterial clearance (A) Inputs for CFU assays. (B) ATG16L1 knock-out HEK293A cells transfected with the indicated HA GST ATG16L1 plasmids were infected with *Salmonella* for 1 hour. Xenophagy rates were examined through CFU assays. Quantification of infection rates by immunofluorescence is demonstrated in the right panel.

Collectively, our data shed light on the relationship between stress and caATG16L1 cleavage showing that: 1) ULK1-mediated phosphorylation of ATG16L1 is increased under infection and starvation, which are known to promote the cleavage of caATG16L1, 2) caATG16L1 is preferentially cleaved upon ULK1 activation, and 3) mutating the ULK1 phosphorylation site reduces ULK1-driven cleavage and improves xenophagy in the caATG16L1 background.

ULK-Mediated Phosphorylation Is Required for ATG16L1 Localization to *Salmonella* and Bacterial Clearance

ULK1 kinase has a well-established role in stimulating autophagy, making it unlikely that the primary function of ULK1-induced ATG16L1 phosphorylation is to activate caspase-mediated cleavage. In order to identify the physiological role of ULK1-mediated ATG16L1 phosphorylation we performed experiments on the wild-type protein, which is not cleaved as readily after phosphorylation. The best described function of ATG16L1 is to promote the correct localization of the E3-like enzyme that lipidates LC3 to the membrane of newly forming autophagosomes. Therefore, we first sought to determine if the localization of pATG16L1 differed from that of total ATG16L1 under infection. To compare localization, we infected MEF with *Salmonella* and immunostained for LPS, pATG16L1, and total ATG16L1. We observed pATG16L1 primarily in the infected samples, confirming the reactivity of our antibody for IF (Fig. 14). Excitingly, we found that pATG16L1 was preferentially localized with internalized bacteria (Fig. 14). Analysis of total ATG16L1 staining also showed co-localization with bacteria, but also contained significantly more diffuse staining in the cytoplasm.

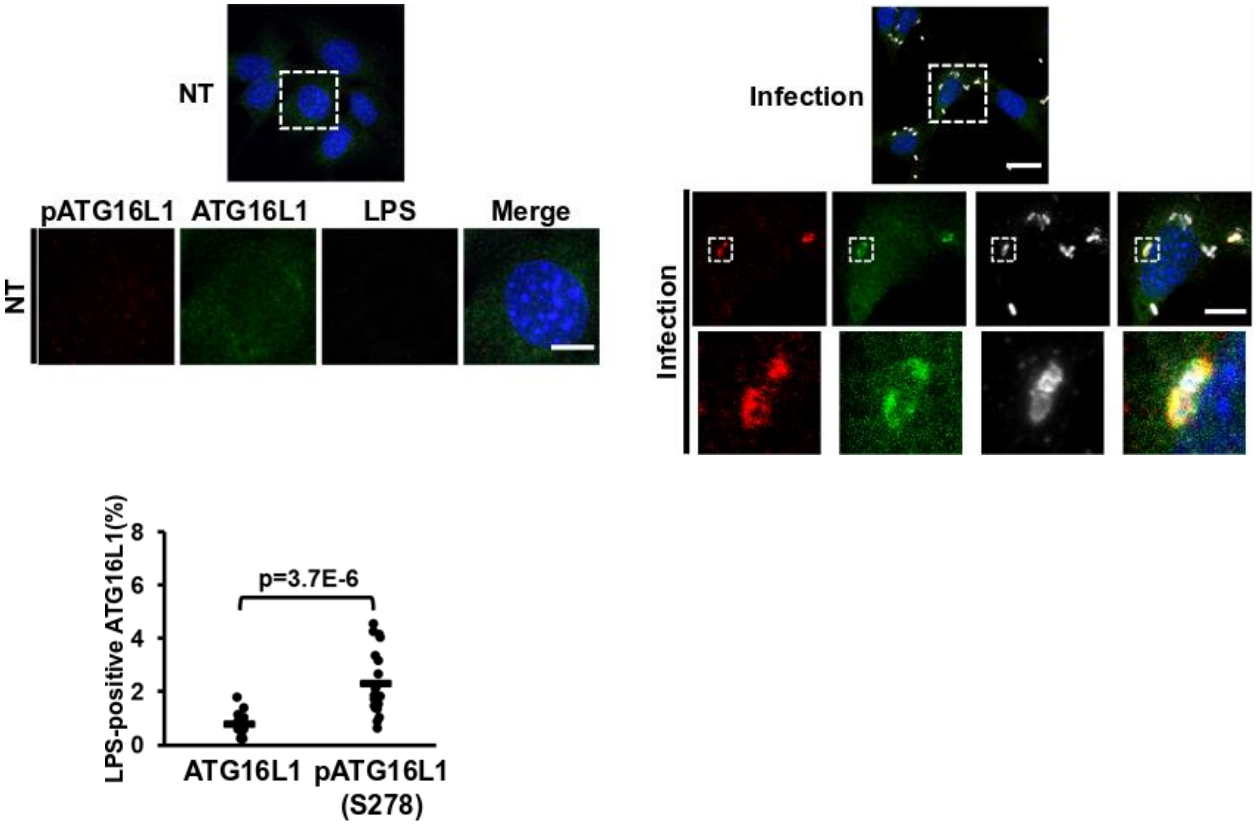

Figure 14: pATG16L1 is specifically localized at the bacterial site. Wild-type cells were infected with *Salmonella* for 1 hour. Phospho-ATG16L1, total ATG16L1, and LPS were stained and analysed by immunofluorescence. Representative immunofluorescent images are shown (scale bars, 10μm).

This could indicate that either ULK1-mediated phosphorylation is important for ATG16L1 recruitment to bacteria, or that the phosphorylation occurs at the bacteria. We reasoned if phosphorylation of ATG16L1 affects bacterial localization then ULK1-deficient cells should exhibit an impairment in ATG16L1 recruitment to pathogen. To test this hypothesis, we infected wild-type or ULK1-deficient cells and quantified the ability of total ATG16L1 to localize to internalized bacteria. Interestingly, we observed that the proportion of ATG16L1-positive bacteria in ULK1-deficient MEF was reduced by over 80% compared to the wild-type controls (Fig. 15).

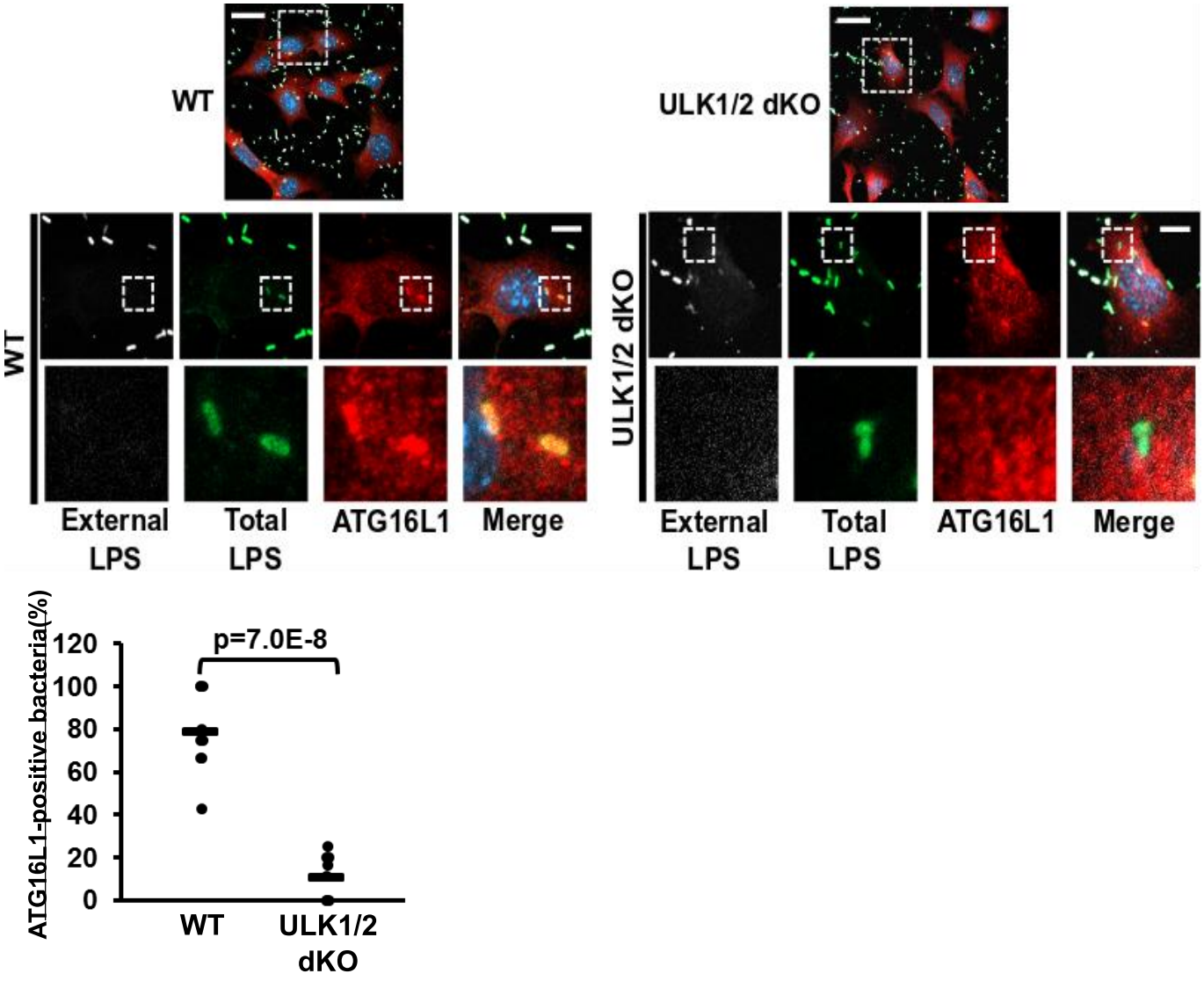

Figure 15: ATG16L1 phosphorylation is required for its localization to bacteria.

Wild-type and ULK dKO were infected with *Salmonella* for 1 hour. Immunofluorescence was performed using antibodies against LPS and ATG16L1. Representative immunofluorescent images are shown on the top panel (scale bars 20μm, 10μm). Quantification of ATG16L1-positive bacteria from 7 fields of view from a representative experiment.

In order to determine the contribution of S278-phosphorylation on ATG16L1 localization to bacteria we reconstituted ATG16L1 KO cells with either wild-type ATG16L1, a truncated form of ATG16L1 that cannot bind the ULK1 complex, or the S278A mutant and analyzed localization to intracellular bacteria. We observed that mutation of S278 or deleting the region of ATG16L1 responsible for binding the ULK1-complex resulted in a significant reduction in ATG16L1-positive bacteria (Fig.16).

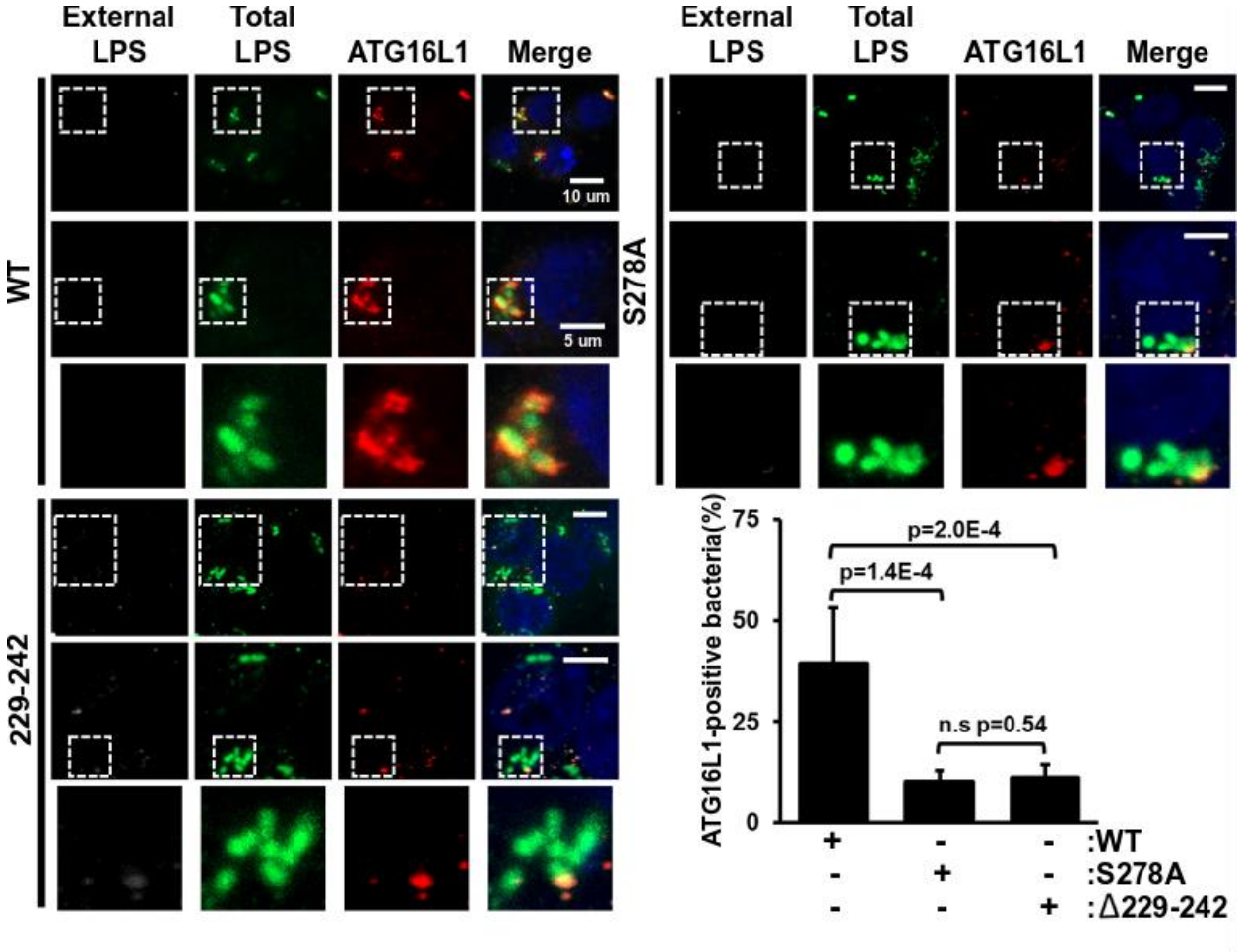

Figure 16: ATG16L1 phosphorylation by ULK is required for its localization to bacteria. ATG16L1 knock-out HCT116 transfected with the indicated GST HA ATG16L1 were infected with *Salmonella* for 1 hour. ATG16L1 (red) puncta was analysed by immunofluorescence (scale bars as indicated).

We then looked at colocalization between LC3B and *Salmonella* in our ATG16L mutants. We observed that the S278A mutant of ATG16L1 in the wildtype background resulted in a reduction in LC3B-positive bacteria (Fig. 17).

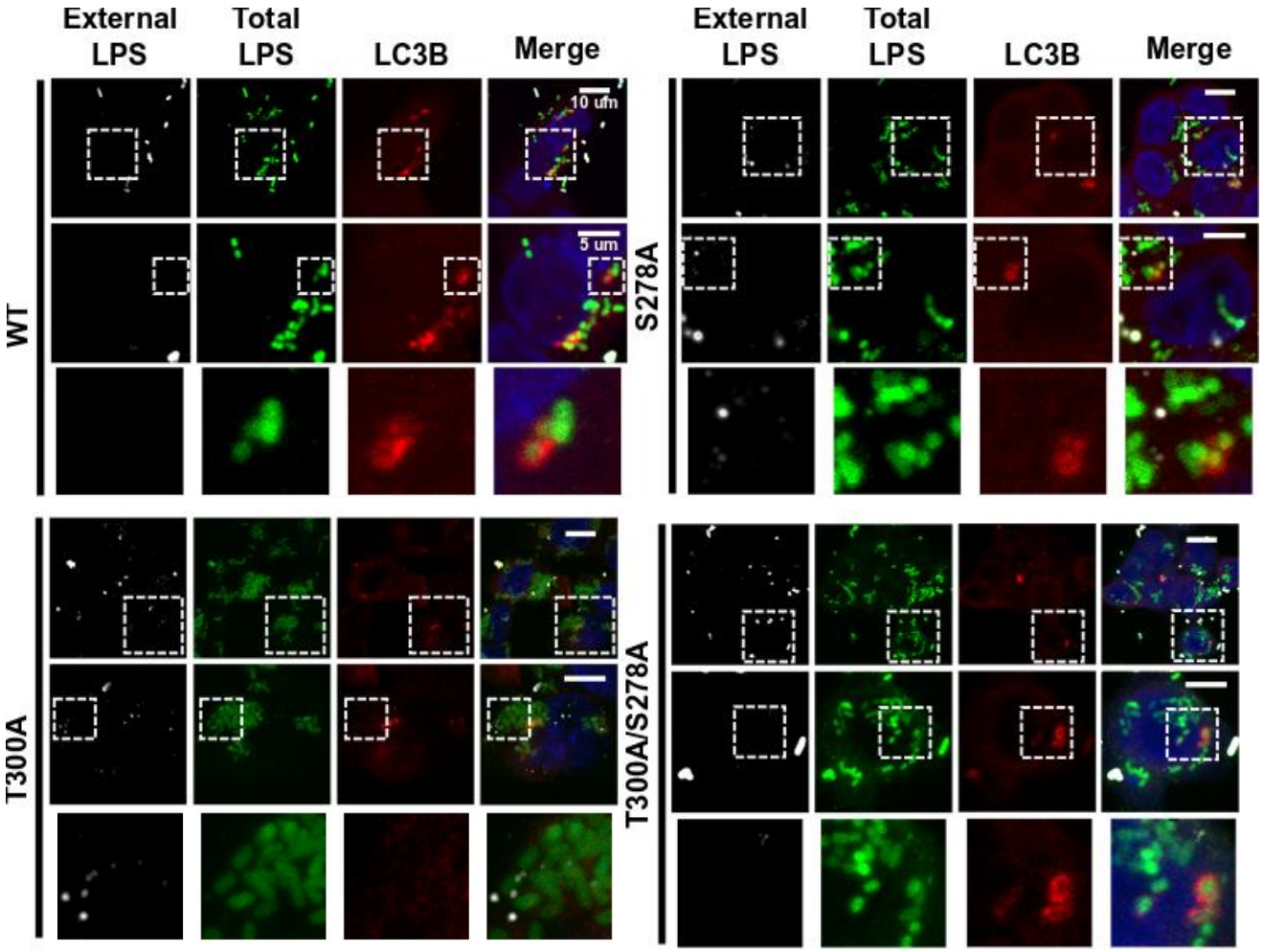

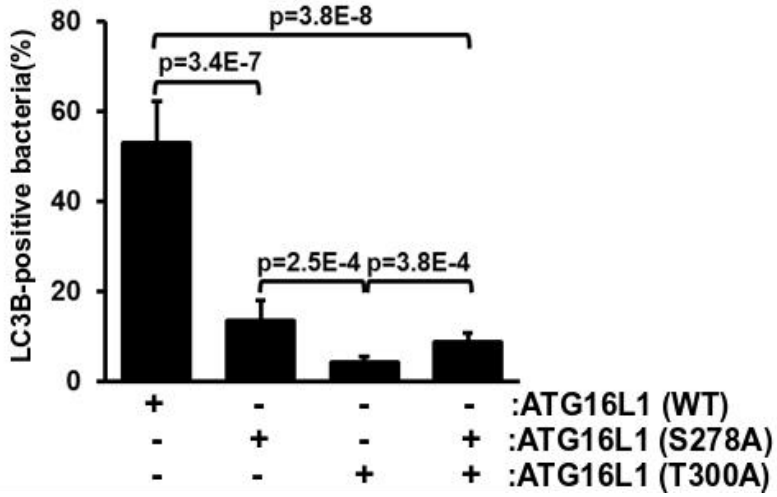

Figure 17: ATG16L1 phosphorylation by ULK is required for LC3 localization to bacteria. HCT116 transfected with the indicated tagged ATG16L1 were infected with *Salmonella* for 1 hour. Bacteria were stained using anti-LPS antibodies to analyze localization in addition to the autophagy marker LC3B. Representative immunofluorescent images of LC3B and LPS are shown in the left panel (scale bars, 5μm). Quantification of bacteria undergoing autophagic clearance from 7 fields of view from a representative experiment is shown in the right panel.

Accordingly, the S278A and truncation mutant of ATG16L1 both were defective in clearing intracellular *Salmonella* as determined by CFU assay (Fig.18). In contrast S278A mutation in the T300A background increased the percentage of LC3B-positive *Salmonella* (Fig. 16), which was also consistent with the decreased bacterial load observed in our CFU assay (Fig13).

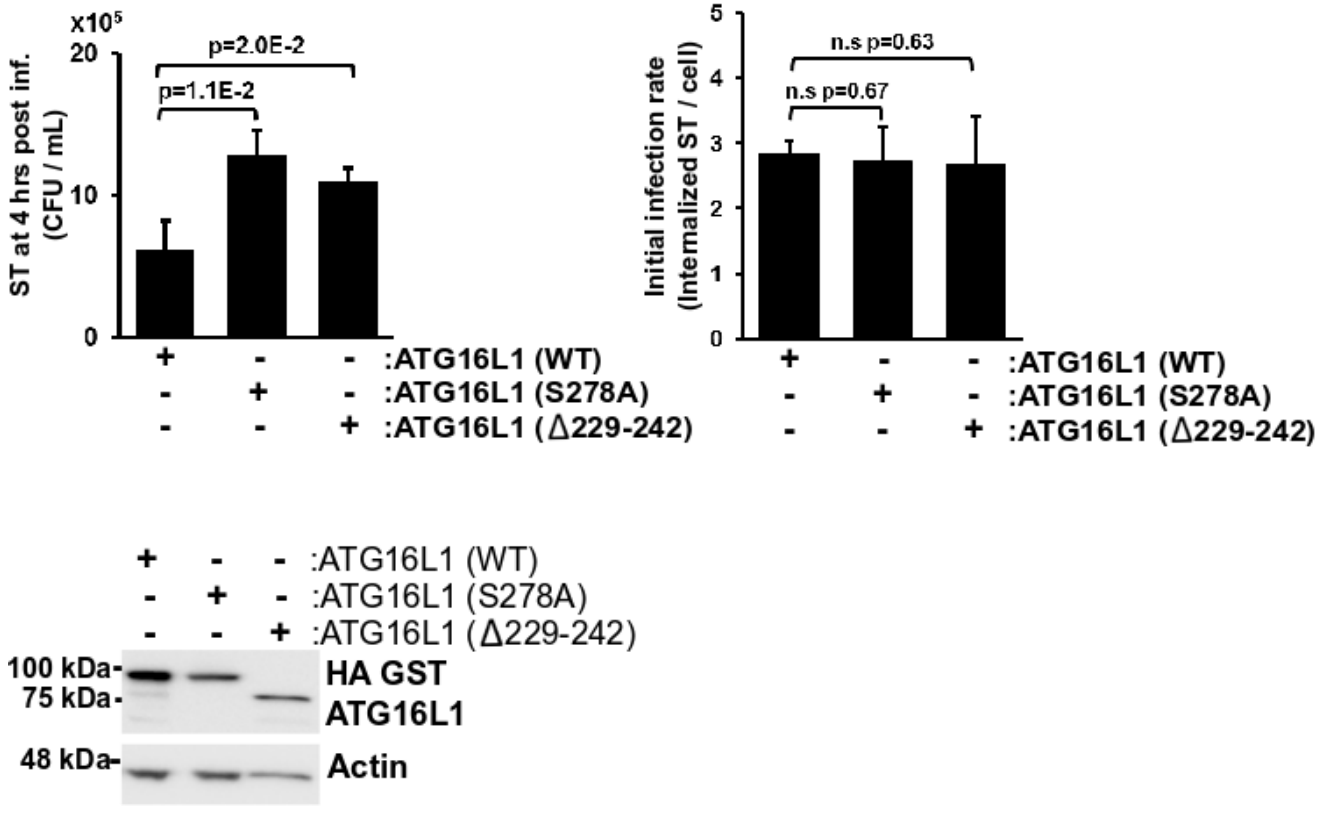

Figure 18: ATG16L1 phosphorylation is required for bacterial clearance ATG16L1 knock-out HEK293A cells transfected with the indicated HA GST ATG16L1 plasmids were infected with *Salmonella* for 1 hour. Xenophagy rates were examined through CFU assays. Quantification of infection rates by immunofluorescence is demonstrated in the middle panel. Expression of ATG16L1 4 hours post infection was examined by WB (right panel).

To determine the role of ULK1-mediated ATG16L1 phosphorylation in starvation we starved cells reconstituted with either wild-type ATG16L1 or ATG16L1(S278A). Surprisingly, we found that S278 mutation had no effect on starvation induced autophagy flux (Fig. 19).

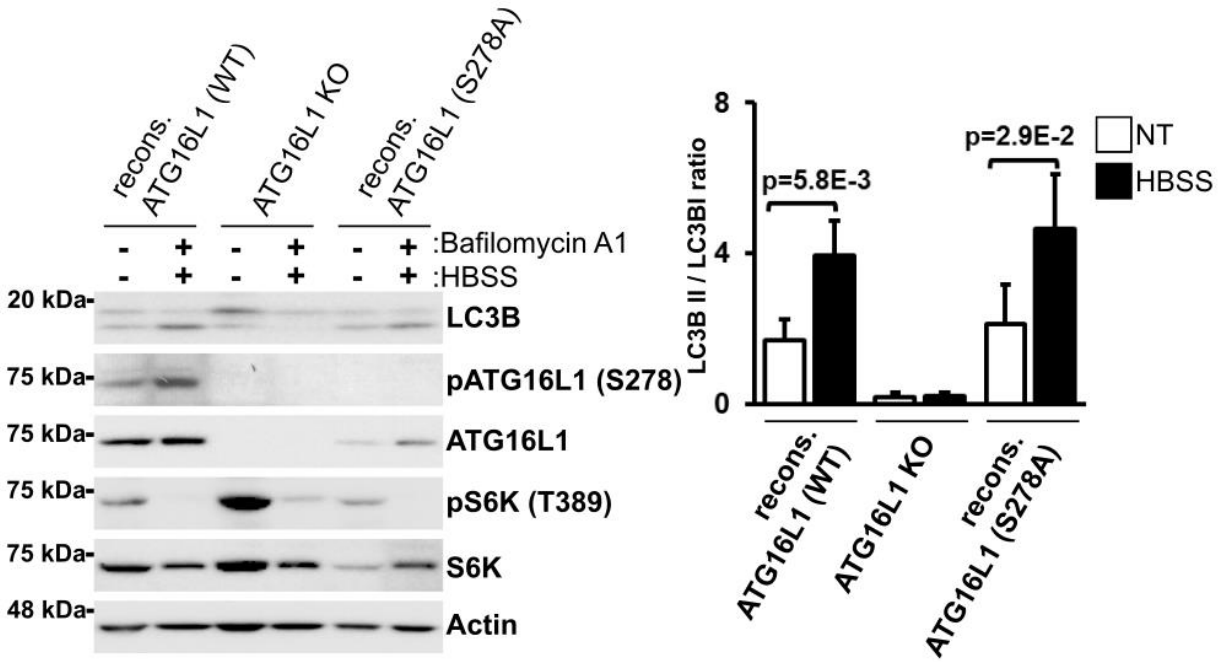

Figure 19: ATG16L1 phosphorylation does not have an effect on starvation induced autophagy flux. ATG16L1 KO HCT116 with or without the indicated reconstituted OLLAS ATG16L1 were incubated with HBSS media in the presence of bafilomycin A1 for 1 hour. LC3B flux was analysed by WB.

These data indicate that either ULK1-mediated phosphorylation of ATG16L1 is more important under infection than starvation or additional functionally redundant signaling pathways to ATG16L1 are activated by starvation. Taken together our data indicate that ULK1-mediated phosphorylation of wild-type ATG16L1 acts to promote localization to internalized bacteria and thereby enhancing bacterial removal, while the same modification is detrimental in caATG16L1 (Fig. 20).

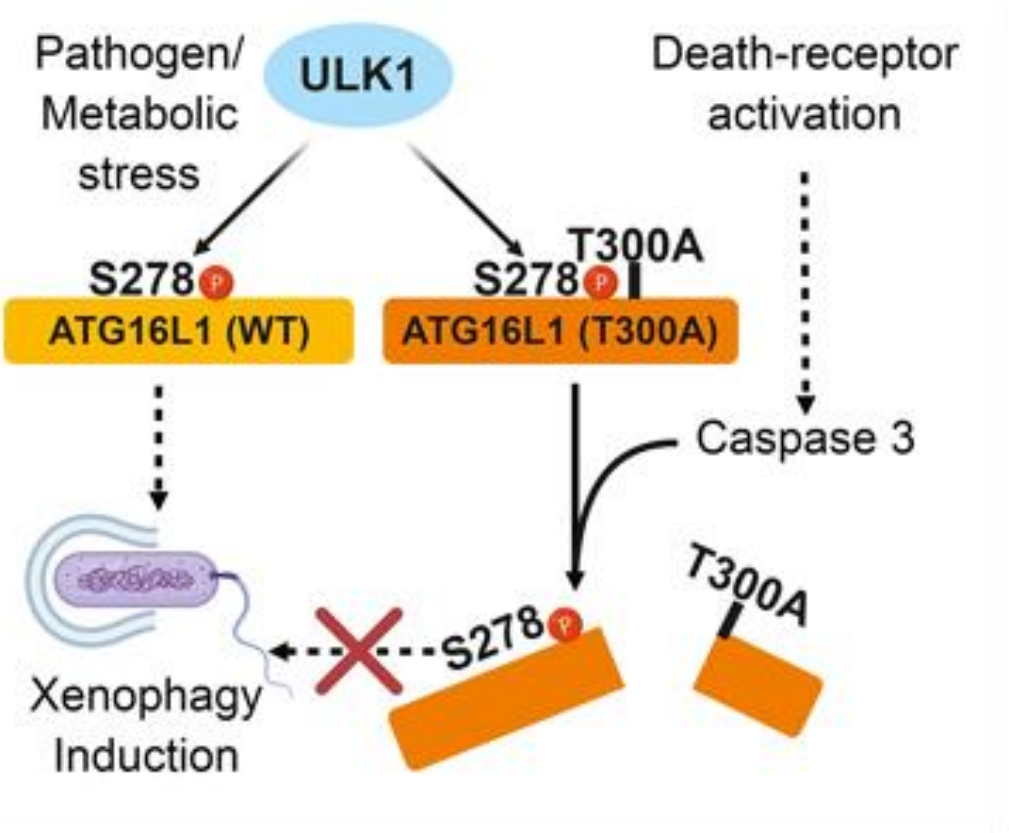

Figure 20: Diagram of the working model demonstrating the dual-role of ULK1-mediated phosphorylation at S278 in wild-type and T300A ATG16L1 background.

Discussion

ULK has previously been described to phosphorylate several components of the autophagy-promoting lipid kinase complex to activate the autophagy pathway[18–20]. Here we have described that the autophagy E3-like enzyme is also regulated by ULK through direct phosphorylation of the ATG16L1 subunit. The discovery of interaction between ULK and the LC3B-lipidating enzyme has raised several interesting lines of inquiry. For example, we have shown that wild-type ATG16L1 is also susceptible to ULK-dependent caspase-mediated cleavage, albeit at a lower level than caATG16L1. However, we currently do not know the physiological relationship between phosphorylation and caspase-mediated cleavage outside the context of the caATG16L1 allele. Potentially, caspase-mediated cleavage of ATG16L1 under stress represents a mechanism to curtail autophagy under severe or prolonged stress. Understanding the mechanistic link between apoptosis and autophagy may yield important conceptual advances.

Genome-wide association studies in the recent years have found a single-nucleotide polymorphism in the autophagy related gene *ATG16L1* that is highly linked with the occurrence of CD[88,89] The mutant polymorphism identified was the T300A allele. ATG16L1 T300A was found to be more susceptible to caspase 3-mediated cleavage, resulting in the degradation and loss of function of ATG16L1, which hindered autophagy activation under stress conditions[61,90]. The region of ATG16L1 which contains the mutated Thr 300 residue has several other putative phosphorlylation sites, but no upstream kinases have been identified to date.

Here we have uncovered a role for ULK-signalling in CD through regulating the stability of caATG16L1. Interestingly, the functional significance of the S278 residue in CD had

already been shown[85]. However, the lack of tools to measure endogenous pATG16L1 resulted in IKKα being identified as the kinase responsible for the phosphorylation and triggering the cleavage of caATG16L1. This is because the initial description of the T300A variant of ATG16L1 showed that Crohn's-associated ATG16L1 is destabilized by stress[61] and is stable under basal conditions. This initial observation is consistent with a stress-inducing ATG16L1 cleavage and has been reproduced by other groups[91] . Indeed, Gao et al found that in cells with wild-type IKKα, TNFα induces cleavage of wild-type ATG16L1[92], which is inconsistent with Diamanti's[85] model which would predict IKK-induced signalling to ATG16L1 would promote stability. Notably, infection and starvation, which can destabilize ATG16L1, are known to activate ULK1[17,93], which is consistent with our model that ULK1-mediated phosphorylation promotes ATG16L1 caspase cleavage in the Crohn's background. These papers and arguments support a stress-induced destabilization model for ATG16L1(T300A), but a relatively simple experiment can address the role of S278 on stability. Diamanti et al proposed that S278A mutation decreases stability similar to T300A (their Fig.5)[85]. Therefore, according to their model one would predict that the double mutant (S278A,T300A) would be even less stable than either individual mutant. However, our model proposes that S278 phosphorylation drives the destabilization of ATG16L1(T300A), which means the double mutant (S278A, T300A) should be more stable if we are correct. We created the ATG16L1 mutations and tested stability in response to ULK1-mediated phosphorylation. We observed that the double mutation of S278A and T300A was significantly more stable than the T300A single mutant (Fig. 11C). Moreover, we found ablating S278 phosphorylation of Crohn's associated ATG16L1 improved anti-bacterial autophagy, which is consistent with our model that

S278 phosphorylation of Crohn's associated ATG16L1 is detrimental (Fig. 13). Our interpretation is that ULK1 is the kinase responsible for ATG16L1 phosphorylation under most conditions. Proving a negative is rarely definitive, so we allow that IKKα could phosphorylate ATG16L1 under some specific set of conditions that we have not tested. However, we would also note IKKα-mediated phosphorylation stated by Diamanti et al was only shown using in vitro kinase assays with purified kinase and substrate that was never verified in cells or endogenously. This assay is notorious in our experience for producing artifacts, as evidenced by the artifactual S287 phosphorylation identified in our mass spec. of an *in vitro* ULK1 kinase assay (Fig. 4). By making the endogenous phospho-antibody against S278 we were able to verify and monitor endogenous regulation of this phosphorylation event on ATG16L1, which only occurs in ULK1/2-containing cells.

Based on our data, as well as the previously reported link between starvation and pathogen-induced caATG16L1 dysfunction, we propose that ULK is the primary kinase responsible for ATG16L1 phosphorylation. However, it is quite possible that IKKα contributes to the destabilization of caATG16L1 through the previously reported activation of caspases[85].

The preferential localization of pATG16L1 to internalized bacteria is another interesting discovery. NOD2 was the first xenophagy related gene identified to be associated to Crohn's disease[94]. Similar to the ATG16L1 T300A polymorphism, NOD2 polymorphisms can result in reduced protein function, which are linked to increased risk of developing CD[95,96]. The recruitment of ATG16L1 to the plasma membrane at the bacteria entry site is facilitated by NOD1 and NOD2 independent of IKK activation[97]. This may imply a

common defect of ATG16L1 function in CD. Consistent with this idea CD-associated SNPs have also been described in ULK1, albeit with less strength than ATG16L1 SNPs. As we have identified a functional redundancy between ULK1 and ULK2 in the promotion of ATG16L1 phosphorylation, which may explain the weak contribution of ULK1 polymorphisms in CD-susceptibility.

Lastly, transcriptional repression of IRGM has also been linked to the development of CD[98]. IRGM has been shown to be essential in defense against intracellular pathogens through activation of autophagy in a cell-autonomous manner[99–101].It has been described as a molecular rheostat that controls the activity of the autophagic process[102]. Since the CD pathophysiology contains a wide range of stress signals which can all contribute to the level of autophagy activation[103,104]. IRGM might play an important role in determining the onset, severity and relapse of CD[105]. Previous studies have investigated the roles of several SNPs of IRGM such as rs13361189 (C>T), rs10065172 (C>T), and rs4958847 (A>G)[106,107], and there has been evidence suggesting that these 3 polymorphisms lead to abnormal expression level of IRGM which ultimately resulted in an increase of susceptibility to CD. Molecularly, IRGM has been shown to bind both ULK1 and ATG16L1, although they have not been shown in a complex together. Therefore, it would be of value to determine if reductions in IRGM protein would have an effect on ULK-mediated ATG16L1 phosphorylation. Clearly, the identification of ULK-mediated ATG16L1 phosphorylation has opened up several avenues for future research, which will undoubtedly expand our understanding of xenophagy and the molecular basis of autophagy defects in CD.

Appendix

Supplemental data

Characterize AMPK and mTORC1 Signalling in The Autophagy Response to Bacterial Infection.

ULK1 activity is strongly regulated via inhibitory phosphorylation by mTORC1 kinase and activating phosphorylation by AMPK[17]. To determine the mechanism by which the host cell detects *Salmonella* regulates AMPK. Mammalian cells have many pattern recognition pathogen recognition receptors (PRRs), which can detect a range of bacterial macromolecules and stimulate the host immune response[108]. The best described receptors are the toll-like receptors (TLRs), which detects LPS, bacterial DNA, or bacterial proteins including flagellin[109]. To determine if stimulation of TLRs was essential for AMPK activation in response to extracellular bacteria we activated the receptors with purified ligands including LPS (activates TLR4) and R848 (activates TLR7/8)[110] as well as viruses (MNV) in a dose-dependent manner. AMPK activation was analysed by Western blot distinctly showed that TLR ligands were not capable of stimulating AMPK signalling (Fig 18).

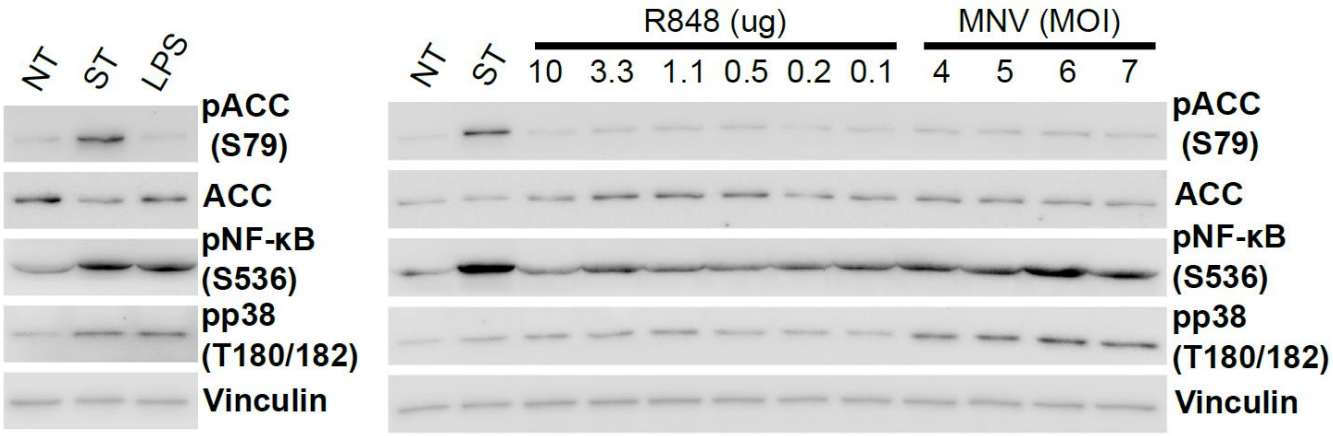

Fig 18. AMPK regulation through TLR receptors MEF cells were infected with *Salmonella* or treated with lipopolysaccharide (LPS, 2 ug/mL), Resiquimod (R848, indicated amounts) and murine noroviruses (MNV, indicated MOI) for 1 hour. Whole cell lysates were immunoblotted using the antibodies indicated.

Characterization of the Molecular Basis of ATG16L1 Phosphorylation by Crohn's Alleles.

Nucleotide-binding oligomerization domain-containing protein 2 (NOD2)

The activation of autophagy can occur due to different cellular stresses such as starvation and infection[104]. It has been established that there is similarity in the regulation of autophagy pathway under starvation and infection (xenophagy)[111]. However, it not completely clear yet. NOD2 senses intracellular microbial pathogens[97]. Previous studies have linked Crohn's disease (CD) with the presence of NOD2 allele leads to increases in the risk of ileal CD[77]. Thus, in our study we attempt to prove the regulation of ATG16L1 phosphorylation by effectors that been linked genetically to CD pathogenesis in response to bacterial infection[78]. We infected both wild type and NOD -/- HCT116 with *Salmonella* for an hour. Interestingly, we found that NOD2 does not promote ATG16L1 phosphorylation at S278 in response to bacterial infection (Fig.19).

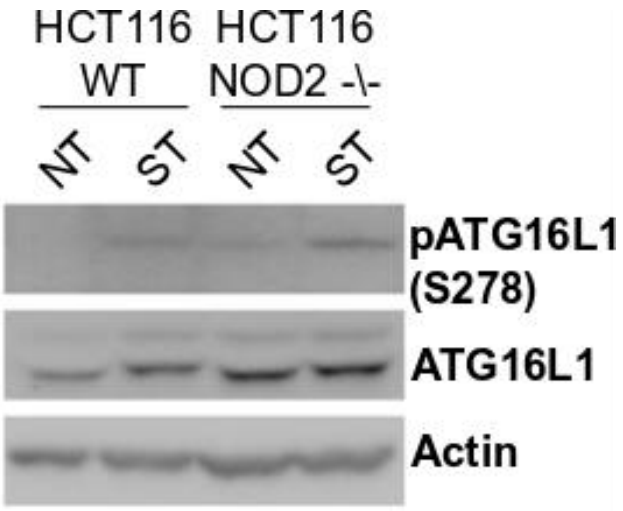

Fig19. ATG16L1 regulation in presents of NOD2. Wild-type and NOD2 KO HCT116, were infected with *salmonella* for an hour. Samples were immunoblotted using the indicated antibodies.

References

1. Parzych, K. R. & Klionsky, D. J. An Overview of Autophagy: Morphology, Mechanism, and Regulation. *Antioxid. Redox Signal.* **20,** 460–473 (2014).

2. Russell, R. C., Yuan, H.-X. & Guan, K.-L. Autophagy regulation by nutrient signaling. *Cell Res.* **24,** 42–57 (2014).

3. Sridhar, S., Botbol, Y., Macian, F. & Cuervo, A. M. Autophagy and Disease: always two sides to a problem. *J. Pathol.* **226,** 255–273 (2012).

4. Harnett, M. M. *et al.* From Christian de Duve to Yoshinori Ohsumi: More to autophagy than just dining at home. *Biomed. J.* **40,** 9–22 (2017).

5. Wang, C.-W. & Klionsky, D. J. The Molecular Mechanism of Autophagy. *Mol. Med.* **9,** 65–76 (2003).

6. Tsukada, M. & Ohsumi, Y. Isolation and characterization of autophagy-defective mutants of Saccharomyces cerevisiae. *FEBS Lett.* **333,** 169–174 (1993).

7. Bernard, A., Jin, M., Xu, Z. & Klionsky, D. J. A large-scale analysis of autophagy-related gene expression identifies new regulators of autophagy. *Autophagy* **11,** 2114–2122 (2015).

8. Wen, X. & Klionsky, D. J. An overview of macroautophagy in yeast. *J. Mol. Biol.* **428,** 1681–1699 (2016).

9. Levine, B. & Klionsky, D. J. Autophagy wins the 2016 Nobel Prize in Physiology or Medicine: Breakthroughs in baker's yeast fuel advances in biomedical research. *Proc. Natl. Acad. Sci.* **114,** 201–205 (2017).

10. Rubinsztein, D. C., Shpilka, T. & Elazar, Z. Mechanisms of Autophagosome Biogenesis. *Curr. Biol.* **22,** R29–R34 (2012).

11. Yang, Z. & Klionsky, D. J. Mammalian autophagy: core molecular machinery and signaling regulation. *Curr. Opin. Cell Biol.* **22,** 124–131 (2010).

12. Jin, M. & Klionsky, D. J. The Core Molecular Machinery of Autophagosome Formation. in *Autophagy and Cancer* (ed. Wang, H.-G.) 25–45 (Springer New York, 2013). doi:10.1007/978-1-4614-6561-4_2

13. Hosokawa, N. *et al.* Nutrient-dependent mTORC1 association with the ULK1-Atg13-FIP200 complex required for autophagy. *Mol. Biol. Cell* **20,** 1981–1991 (2009).

14. Jung, C. H. *et al.* ULK-Atg13-FIP200 complexes mediate mTOR signaling to the autophagy machinery. *Mol. Biol. Cell* **20,** 1992–2003 (2009).

15. Suzuki, H., Osawa, T., Fujioka, Y. & Noda, N. N. Structural biology of the core autophagy machinery. *Curr. Opin. Struct. Biol.* **43,** 10–17 (2017).

16. Ahmad, S. T. & Lee, J.-A. *Autophagy: Chapter 3. Molecular Mechanisms Underlying the Role of Autophagy in Neurodegenerative Diseases*. (Elsevier Inc. Chapters, 2013).

17. Kim, J., Kundu, M., Viollet, B. & Guan, K.-L. AMPK and mTOR regulate autophagy through direct phosphorylation of Ulk1. *Nat. Cell Biol.* **13,** 132–141 (2011).

18. Russell, R. C. *et al.* ULK1 induces autophagy by phosphorylating Beclin-1 and activating Vps34 lipid kinase. *Nat. Cell Biol.* **15,** 741–750 (2013).

19. Di Bartolomeo, S. *et al.* The dynamic interaction of AMBRA1 with the dynein motor complex regulates mammalian autophagy. *J. Cell Biol.* **191,** 155–168 (2010).

20. Park, J.-M. *et al.* The ULK1 complex mediates MTORC1 signaling to the autophagy initiation machinery via binding and phosphorylating ATG14. *Autophagy* **12,** 547–564 (2016).

21. Fan, W., Nassiri, A. & Zhong, Q. Autophagosome targeting and membrane curvature sensing by Barkor/Atg14(L). *Proc. Natl. Acad. Sci.* **108,** 7769–7774 (2011).

22. Yuan, H.-X., Russell, R. C. & Guan, K.-L. Regulation of PIK3C3/VPS34 complexes by MTOR in nutrient stress-induced autophagy. *Autophagy* **9,** 1983–1995 (2013).

23. Fujita, N. *et al.* The Atg16L complex specifies the site of LC3 lipidation for membrane biogenesis in autophagy. *Mol. Biol. Cell* **19,** 2092–2100 (2008).

24. Mizushima, N. *et al.* A protein conjugation system essential for autophagy. *Nature* **395,** 395–398 (1998).

25. Hardie, D. G. AMP-activated protein kinase—an energy sensor that regulates all aspects of cell function. *Genes Dev.* **25,** 1895–1908 (2011).

26. Velden, Y. U. van der *et al.* The serine-threonine kinase LKB1 is essential for survival under energetic stress in zebrafish. *Proc. Natl. Acad. Sci.* **108,** 4358–4363 (2011).

27. Shackelford, D. B. & Shaw, R. J. The LKB1-AMPK pathway: metabolism and growth control in tumor suppression. *Nat. Rev. Cancer* **9,** 563–575 (2009).

28. Burman, C. & Ktistakis, N. T. Regulation of autophagy by phosphatidylinositol 3-phosphate. *FEBS Lett.* **584,** 1302–1312 (2010).

29. Zachari, M. & Ganley, I. G. The mammalian ULK1 complex and autophagy initiation. *Essays Biochem.* **61,** 585–596 (2017).

30. Kim, J. *et al.* Differential regulation of distinct Vps34 complexes by AMPK in nutrient stress and autophagy. *Cell* **152,** 290–303 (2013).

31. Morris, D. H., Yip, C. K., Shi, Y., Chait, B. T. & Wang, Q. J. BECLIN 1-VPS34 COMPLEX ARCHITECTURE: UNDERSTANDING THE NUTS AND BOLTS OF THERAPEUTIC TARGETS. *Front. Biol.* **10,** 398–426 (2015).

32. Sun, Q., Westphal, W., Wong, K. N., Tan, I. & Zhong, Q. Rubicon controls endosome maturation as a Rab7 effector. *Proc. Natl. Acad. Sci. U. S. A.* **107,** 19338–19343 (2010).

33. Young, A. R. J. *et al.* Starvation and ULK1-dependent cycling of mammalian Atg9 between the TGN and endosomes. *J. Cell Sci.* **119,** 3888–3900 (2006).

34. Lang, T., Reiche, S., Straub, M., Bredschneider, M. & Thumm, M. Autophagy and the cvt Pathway Both Depend on AUT9. *J. Bacteriol.* **182,** 2125–2133 (2000).

35. Noda, T. *et al.* Apg9p/Cvt7p is an integral membrane protein required for transport vesicle formation in the Cvt and autophagy pathways. *J. Cell Biol.* **148,** 465–480 (2000).

36. Zhuang, X. *et al.* ATG9 regulates autophagosome progression from the endoplasmic reticulum in Arabidopsis. *Proc. Natl. Acad. Sci. U. S. A.* **114,** E426–E435 (2017).

37. Molejon, M. I., Ropolo, A., Re, A. L., Boggio, V. & Vaccaro, M. I. The VMP1-Beclin 1 interaction regulates autophagy induction. *Sci. Rep.* **3,** (2013).

38. Molejon, M. I., Ropolo, A. & Vaccaro, M. I. VMP1 is a new player in the regulation of the autophagy-specific phosphatidylinositol 3-kinase complex activation. *Autophagy* **9,** 933–935 (2013).

39. Müller, A. J. & Proikas-Cezanne, T. Function of human WIPI proteins in autophagosomal rejuvenation of endomembranes? *FEBS Lett.* **589,** 1546–1551 (2015).

40. Grimmel, M., Backhaus, C. & Proikas-Cezanne, T. WIPI-Mediated Autophagy and Longevity. *Cells* **4,** 202–217 (2015).

41. Carlsson, S. R. & Simonsen, A. Membrane dynamics in autophagosome biogenesis. *J Cell Sci* **128,** 193–205 (2015).

42. WIPI2 Links LC3 Conjugation with PI3P, Autophagosome Formation, and Pathogen Clearance by Recruiting Atg12–5-16L1. Available at: https://www.ncbi.nlm.nih.gov/pmc/articles/PMC4104028/. (Accessed: 21st September 2018)

43. Nakatogawa, H. Two ubiquitin-like conjugation systems that mediate membrane formation during autophagy. *Essays Biochem.* **55,** 39–50 (2013).

44. Walczak, M. & Martens, S. Dissecting the role of the Atg12-Atg5-Atg16 complex during autophagosome formation. *Autophagy* **9,** 424–425 (2013).

45. Geng, J. & Klionsky, D. J. The Atg8 and Atg12 ubiquitin-like conjugation systems in macroautophagy. 'Protein Modifications: Beyond the Usual Suspects'' Review Series'. *EMBO Rep.* **9,** 859–864 (2008).

46. Tanida, I., Ueno, T. & Kominami, E. LC3 conjugation system in mammalian autophagy. *Int. J. Biochem. Cell Biol.* **36,** 2503–2518 (2004).

47. Johansen, T. & Lamark, T. Selective autophagy mediated by autophagic adapter proteins. *Autophagy* **7,** 279–296 (2011).

48. Gao, W., Chen, Z., Wang, W. & Stang, M. T. E1-Like Activating Enzyme Atg7 Is Preferentially Sequestered into p62 Aggregates via Its Interaction with LC3-I. *PLoS ONE* **8,** (2013).

49. Zaffagnini, G. & Martens, S. Mechanisms of Selective Autophagy. *J. Mol. Biol.* **428,** 1714–1724 (2016).

50. Schreiber, A. & Peter, M. Substrate recognition in selective autophagy and the ubiquitin–proteasome system. *Biochim. Biophys. Acta BBA - Mol. Cell Res.* **1843,** 163–181 (2014).

51. Svenning, S. & Johansen, T. Selective autophagy. *Essays Biochem.* **55,** 79–92 (2013).

52. Lamark, T. & Johansen, T. Aggrephagy: Selective Disposal of Protein Aggregates by Macroautophagy. *International Journal of Cell Biology* (2012). doi:10.1155/2012/736905

53. Grootjans, J., Kaser, A., Kaufman, R. J. & Blumberg, R. S. The unfolded protein response in immunity and inflammation. *Nat. Rev. Immunol.* **16,** 469–484 (2016).

54. Lim, J. & Yue, Z. Neuronal aggregates: formation, clearance and spreading. *Dev. Cell* **32,** 491–501 (2015).

55. Lippai, M. & Lőw, P. The Role of the Selective Adaptor p62 and Ubiquitin-Like Proteins in Autophagy. *BioMed Research International* (2014). doi:10.1155/2014/832704

56. Manley, S., Williams, J. A. & Ding, W.-X. The Role of p62/SQSTM1 in Liver Physiology and Pathogenesis. *Exp. Biol. Med. Maywood NJ* **238,** 525–538 (2013).

57. Jo, E.-K., Yuk, J.-M., Shin, D.-M. & Sasakawa, C. Roles of Autophagy in Elimination of Intracellular Bacterial Pathogens. *Front. Immunol.* **4,** (2013).

58. Intracellular recognition of pathogens and autophagy as an innate immune host defence | The Journal of Biochemistry | Oxford Academic. Available at: https://academic.oup.com/jb/article/150/2/143/2182733. (Accessed: 21st September 2018)

59. Randow, F. & Youle, R. J. Self and nonself: how autophagy targets mitochondria and bacteria. *Cell Host Microbe* **15,** 403–411 (2014).

60. Chauhan, S., Mandell, M. A. & Deretic, V. IRGM governs the core autophagy machinery to conduct antimicrobial defense. *Mol. Cell* **58,** 507–521 (2015).

61. Murthy, A. *et al.* A Crohn's disease variant in Atg16l1 enhances its degradation by caspase 3. *Nature* **506,** 456–462 (2014).

62. Maiuri, M. C., Zalckvar, E., Kimchi, A. & Kroemer, G. Self-eating and self-killing: crosstalk between autophagy and apoptosis. *Nat. Rev. Mol. Cell Biol.* **8,** 741–752 (2007).

63. Kroemer, G., Mariño, G. & Levine, B. Autophagy and the integrated stress response. *Mol. Cell* **40,** 280–293 (2010).

64. Nuñez, G., Benedict, M. A., Hu, Y. & Inohara, N. Caspases: the proteases of the apoptotic pathway. *Oncogene* **17,** 3237–3245 (1998).

65. Mariño, G., Niso-Santano, M., Baehrecke, E. H. & Kroemer, G. Self-consumption: the interplay of autophagy and apoptosis. *Nat. Rev. Mol. Cell Biol.* **15,** 81–94 (2014).

66. Levine, B. & Kroemer, G. Autophagy in the Pathogenesis of Disease. *Cell* **132,** 27–42 (2008).

67. Yue, Z., Jin, S., Yang, C., Levine, A. J. & Heintz, N. Beclin 1, an autophagy gene essential for early embryonic development, is a haploinsufficient tumor suppressor. *Proc. Natl. Acad. Sci. U. S. A.* **100,** 15077–15082 (2003).

68. Sweeney, P. *et al.* Protein misfolding in neurodegenerative diseases: implications and strategies. *Transl. Neurodegener.* **6,** (2017).

69. Jaeger, P. A. & Wyss-Coray, T. All-you-can-eat: autophagy in neurodegeneration and neuroprotection. *Mol. Neurodegener.* **4,** 16 (2009).

70. Schulte, J. & Littleton, J. T. The biological function of the Huntingtin protein and its relevance to Huntington's Disease pathology. *Curr. Trends Neurol.* **5,** 65–78 (2011).

71. Abd-Elrahman, K. S. *et al.* mGluR5 antagonism increases autophagy and prevents disease progression in the zQ175 mouse model of Huntington's disease. *Sci Signal* **10,** eaan6387 (2017).

72. Mei, Y., Thompson, M. D., Cohen, R. A. & Tong, X. Autophagy and oxidative stress in cardiovascular diseases. *Biochim. Biophys. Acta BBA - Mol. Basis Dis.* **1852,** 243–251 (2015).

73. The role of autophagy in cardiomyocytes in the basal state and in response to hemodynamic stress | Nature Medicine. Available at: https://www.nature.com/articles/nm1574. (Accessed: 21st September 2018)

74. Freeman, H. J. Natural history and long-term clinical course of Crohn's disease. *World J. Gastroenterol.* **20,** 31–36 (2014).

75. Hendrickson, B. A., Gokhale, R. & Cho, J. H. Clinical Aspects and Pathophysiology of Inflammatory Bowel Disease. *Clin. Microbiol. Rev.* **15,** 79–94 (2002).

76. M'Koma, A. E. Inflammatory Bowel Disease: An Expanding Global Health Problem. *Clin. Med. Insights Gastroenterol.* **6,** 33–47 (2013).

77. Petersen, H. J. & Smith, A. M. The Role of the Innate Immune System in Granulomatous Disorders. *Front. Immunol.* **4,** (2013).

78. Huttenhower, C., Kostic, A. D. & Xavier, R. J. Inflammatory bowel disease as a model for translating the microbiome. *Immunity* **40,** 843–854 (2014).

79. Brest, P. *et al.* Autophagy and Crohn's Disease: At the Crossroads of Infection, Inflammation, Immunity, and Cancer. *Curr. Mol. Med.* **10,** 486 (2010).

80. Evidence from Genetics for a Role of Autophagy and Innate Immunity in IBD Pathogenesis - Abstract - Digestive Diseases 2012, Vol. 30, No. 4 - Karger Publishers. Available at: https://www.karger.com/Article/Abstract/338119. (Accessed: 21st September 2018)

81. Massey, D. C. O. & Parkes, M. Genome-wide association scanning highlights two autophagy genes, ATG16L1 and IRGM, as being significantly associated with Crohn's disease. *Autophagy* **3,** 649–651 (2007).

82. Sadaghian Sadabad, M. *et al.* The ATG16L1-T300A allele impairs clearance of pathosymbionts in the inflamed ileal mucosa of Crohn's disease patients. *Gut* **64,** 1546–1552 (2015).

83. Sorbara, M. T. *et al.* The protein ATG16L1 suppresses inflammatory cytokines induced by the intracellular sensors Nod1 and Nod2 in an autophagy-independent manner. *Immunity* **39,** 858–873 (2013).

84. Homer, C. R., Richmond, A. L., Rebert, N. A., Achkar, J.-P. & McDonald, C. ATG16L1 and NOD2 interact in an autophagy-dependent antibacterial pathway implicated in Crohn's disease pathogenesis. *Gastroenterology* **139,** 1630–1641, 1641.e1–2 (2010).

85. Diamanti, M. A. *et al.* IKKα controls ATG16L1 degradation to prevent ER stress during inflammation. *J. Exp. Med.* **214,** 423–437 (2017).

86. Gao, P. *et al.* The Inflammatory Bowel Disease-Associated Autophagy Gene Atg16L1T300A Acts as a Dominant Negative Variant in Mice. *J. Immunol. Baltim. Md 1950* **198,** 2457–2467 (2017).

87. The T300A Crohn's disease risk polymorphism impairs function of the WD40 domain of ATG16L1 | Nature Communications. Available at: https://www.nature.com/articles/ncomms11821. (Accessed: 21st September 2018)

88. Hampe, J. *et al.* A genome-wide association scan of nonsynonymous SNPs identifies a susceptibility variant for Crohn disease in ATG16L1. *Nat. Genet.* **39,** 207–211 (2007).

89. Rioux, L.-E., Turgeon, S. L. & Beaulieu, M. Characterization of polysaccharides extracted from brown seaweeds. *Carbohydr. Polym.* **69,** 530–537 (2007).

90. Lassen, K. G. *et al.* Atg16L1 T300A variant decreases selective autophagy resulting in altered cytokine signaling and decreased antibacterial defense. *Proc. Natl. Acad. Sci.* **111,** 7741–7746 (2014).

91. Fang, R. *et al.* NEMO-IKKβ Are Essential for IRF3 and NF-κB Activation in the cGAS-STING Pathway. *J. Immunol. Baltim. Md 1950* **199,** 3222–3233 (2017).

92. Gao, Z. *et al.* Serine phosphorylation of insulin receptor substrate 1 by inhibitor kappa B kinase complex. *J. Biol. Chem.* **277,** 48115–48121 (2002).

93. Losier, T. T. *et al.* AMPK Promotes Xenophagy through Priming of Autophagic Kinases upon Detection of Bacterial Outer Membrane Vesicles. *Cell Rep.* **26,** 2150-2165.e5 (2019).

94. A frameshift mutation in NOD2 associated with susceptibility to Crohn's disease | Nature. Available at: https://www.nature.com/articles/35079114. (Accessed: 22nd March 2019)

95. Hugot, J. P. *et al.* Association of NOD2 leucine-rich repeat variants with susceptibility to Crohn's disease. *Nature* **411,** 599–603 (2001).

96. Wehkamp, J. *et al.* NOD2 (CARD15) mutations in Crohn's disease are associated with diminished mucosal alpha-defensin expression. *Gut* **53,** 1658–1664 (2004).

97. Travassos, L. H. *et al.* Nod1 and Nod2 direct autophagy by recruiting ATG16L1 to the plasma membrane at the site of bacterial entry. *Nat. Immunol.* **11,** 55–62 (2010).

98. Murdoch, T. B. *et al.* Pattern recognition receptor and autophagy gene variants are associated with development of antimicrobial antibodies in Crohn's disease. *Inflamm. Bowel Dis.* **18,** 1743–1748 (2012).

99. The IRG protein-based resistance mechanism in mice and its relation to virulence in Toxoplasma gondii - ScienceDirect. Available at: https://www.sciencedirect.com/science/article/pii/S1369527411000865. (Accessed: 20th March 2019)

100. Lapaquette, P., Brest, P., Hofman, P. & Darfeuille-Michaud, A. Etiology of Crohn's disease: many roads lead to autophagy. *J. Mol. Med. Berl. Ger.* **90,** 987–996 (2012).

101. Deretic, V. Autophagy as an innate immunity paradigm: expanding the scope and repertoire of pattern recognition receptors. *Curr. Opin. Immunol.* **24,** 21–31 (2012).

102. Folmes, C. D. L., Dzeja, P. P., Nelson, T. J. & Terzic, A. Metabolic plasticity in stem cell homeostasis and differentiation. *Cell Stem Cell* **11,** 596–606 (2012).

103. Caramés, B., Taniguchi, N., Otsuki, S., Blanco, F. J. & Lotz, M. Autophagy is a protective mechanism in normal cartilage, and its aging-related loss is linked with cell death and osteoarthritis. *Arthritis Rheum.* **62,** 791–801 (2010).

104. Deretic, V., Saitoh, T. & Akira, S. Autophagy in infection, inflammation and immunity. *Nat. Rev. Immunol.* **13,** 722–737 (2013).

105. Lapaquette, P., Glasser, A.-L., Huett, A., Xavier, R. J. & Darfeuille-Michaud, A. Crohn's disease-associated adherent-invasive E. coli are selectively favoured by impaired autophagy to replicate intracellularly. *Cell. Microbiol.* **12,** 99–113 (2010).

106. Waterman, M. *et al.* Distinct and Overlapping Genetic Loci in Crohn's Disease and Ulcerative Colitis: Correlations with Pathogenesis. *Inflamm. Bowel Dis.* **17,** 1936–1942 (2011).

107. Moon, C. M. *et al.* Associations Between Genetic Variants in the IRGM Gene and Inflammatory Bowel Diseases in the Korean Population. *Inflamm. Bowel Dis.* **19,** 106–114 (2013).

108. Mogensen, T. H. Pathogen Recognition and Inflammatory Signaling in Innate Immune Defenses. *Clin. Microbiol. Rev.* **22,** 240–273 (2009).

109. Janssens, S. & Beyaert, R. Role of Toll-Like Receptors in Pathogen Recognition. *Clin. Microbiol. Rev.* **16,** 637–646 (2003).

110. Hofmann, H., Vanwalscappel, B., Bloch, N. & Landau, N. R. TLR7/8 agonist induces a post-entry SAMHD1-independent block to HIV-1 infection of monocytes. *Retrovirology* **13,** (2016).

111. Bauckman, K. A., Owusu-Boaitey, N. & Mysorekar, I. U. Selective Autophagy: Xenophagy. *Methods San Diego Calif* **75,** 120–127 (2015).

Copy Rights

This Agreement between University of Ottawa -- Reham Alsaadi ("You") and Springer Nature ("Springer Nature") consists of your license details and the terms and conditions provided by Springer Nature and Copyright Clearance Center.

License Number	4546710864131
License date	Mar 12, 2019
Licensed Content Publisher	Springer Nature
Licensed Content Publication	Springer eBook
Licensed Content Title	The Core Molecular Machinery of Autophagosome Formation
Licensed Content Author	Meiyan Jin, Daniel J. Klionsky
Licensed Content Date	Jan 1, 2013
Type of Use	Thesis/Dissertation
Requestor type	academic/university or research institute
Format	print and electronic
Portion	figures/tables/illustrations
Number of figures/tables/illustrations	1
Will you be translating?	no
Circulation/distribution	<501

Author of this Springer Nature content	no
Title	Characterization of post-translational modification of ATG16L1 in antibacterial autophagy
Institution name	university of ottawa
Expected presentation date	Mar 2019
Portions	1 Table (Table 2.1)
Requestor Location	University of Ottawa 451 Smyth Rd, Ottawa, ON K1H 8L1 Apt 108 Ottawa, ON K1H 8L1 Canada Attn: University of Ottawa
Billing Type	Invoice
Billing Address	University of Ottawa 451 Smyth Rd, Ottawa, ON K1H 8L1 Apt 108 Ottawa, ON K1H 8L1 Canada Attn: University of Ottawa
Total	0.00 USD
Terms and Conditions	

Springer Nature Terms and Conditions for RightsLink Permissions

Springer Nature Customer Service Centre GmbH (the Licensor) hereby grants you a non-exclusive, world-wide licence to reproduce the material and for the purpose and requirements specified in the attached copy of your order form, and for no other use, subject to the conditions below:

1. The Licensor warrants that it has, to the best of its knowledge, the rights to license reuse of this material. However, you should ensure that the material you are requesting is original to the Licensor and does not carry the copyright of another entity (as credited in the published version).

   If the credit line on any part of the material you have requested indicates that it was reprinted or adapted with permission from another source, then you should also seek permission from that source to reuse the material.

2. Where **print only** permission has been granted for a fee, separate permission must be obtained for any additional electronic re-use.

3. Permission granted **free of charge** for material in print is also usually granted for any electronic version of that work, provided that the material is incidental to your work as a whole and that the electronic version is essentially equivalent to, or substitutes for, the print version.

4. A licence for 'post on a website' is valid for 12 months from the licence date. This licence does not cover use of full text articles on websites.

5. Where **'reuse in a dissertation/thesis'** has been selected the following terms apply: Print rights of the final author's accepted manuscript (for clarity, NOT the published version) for up to 100 copies, electronic rights for use only on a personal website or institutional repository as defined by the Sherpa guideline (www.sherpa.ac.uk/romeo/).

6. Permission granted for books and journals is granted for the lifetime of the first edition and does not apply to second and subsequent editions (except where the first edition permission was granted free of charge or for signatories to the STM Permissions Guidelines http://www.stm-assoc.org/copyright-legal-affairs/permissions/permissions-guidelines/), and does not apply for editions in other languages unless additional translation rights have been granted separately in the licence.

7. Rights for additional components such as custom editions and derivatives require additional permission and may be subject to an additional fee. Please apply to Journalpermissions@springernature.com/bookpermissions@springernature.com for these rights.

8. The Licensor's permission must be acknowledged next to the licensed material in print. In electronic form, this acknowledgement must be visible at the same

time as the figures/tables/illustrations or abstract, and must be hyperlinked to the journal/book's homepage. Our required acknowledgement format is in the Appendix below.

9. Use of the material for incidental promotional use, minor editing privileges (this does not include cropping, adapting, omitting material or any other changes that affect the meaning, intention or moral rights of the author) and copies for the disabled are permitted under this licence.

10. Minor adaptations of single figures (changes of format, colour and style) do not require the Licensor's approval. However, the adaptation should be credited as shown in Appendix below.

Appendix — Acknowledgements:

For Journal Content:

Reprinted by permission from [**the Licensor**]: [**Journal Publisher** (e.g. Nature/Springer/Palgrave)] [**JOURNAL NAME**] [**REFERENCE CITATION**(Article name, Author(s) Name), [**COPYRIGHT**] (year of publication)

For **Advance Online Publication papers:**

Reprinted by permission from [**the Licensor**]: [**Journal Publisher** (e.g. Nature/Springer/Palgrave)] [**JOURNAL NAME**] [**REFERENCE CITATION**(Article name, Author(s) Name), [**COPYRIGHT**] (year of publication), advance online publication, day month year (doi: 10.1038/sj.[JOURNAL ACRONYM].)

For Adaptations/Translations:

Adapted/Translated by permission from [**the Licensor**]: [**Journal Publisher** (e.g. Nature/Springer/Palgrave)] [**JOURNAL NAME**] [**REFERENCE CITATION**(Article name, Author(s) Name), [**COPYRIGHT**] (year of publication)

Note: For any republication from the British Journal of Cancer, the following credit line style applies:

Reprinted/adapted/translated by permission from [**the Licensor**]: on behalf of Cancer Research UK: : [**Journal Publisher** (e.g. Nature/Springer/Palgrave)] [**JOURNAL NAME**] [**REFERENCE CITATION** (Article name, Author(s) Name), [**COPYRIGHT]** (year of publication)

For **Advance Online Publication** papers:

Reprinted by permission from The [**the Licensor**]: on behalf of Cancer Research UK: [**Journal Publisher** (e.g. Nature/Springer/Palgrave)] [**JOURNAL NAME**] [**REFERENCE CITATION** (Article name, Author(s) Name), [**COPYRIGHT**] (year of publication), advance online publication, day month year (doi: 10.1038/sj.[JOURNAL ACRONYM])

For Book content:

Reprinted/adapted by permission from [**the Licensor**]: [**Book Publisher** (e.g. Palgrave Macmillan, Springer etc) [**Book Title**] by [**Book author**(s)] [**COPYRIGHT**] (year of publication)

Other Conditions:

Version 1.1

Questions? customercare@copyright.com or +1-855-239-3415 (toll free in the US) or +1-978-646-2777.